Please note that this is an author-produced PDF of an article accepted for publication following peer review. The definitive publisher-authenticated version is available on the publisher Web site

Marine Geology
November 2007, Volume 245, Issues 1-4, Pages 65-88
http://dx.doi.org/10.1016/j.margeo.2007.07.006
© 2007 Elsevier B.V. All rights reserved.

Archimer
Archive Institutionnelle de l'Ifremer
http://www.ifremer.fr/docelec/

Late Glacial to Preboreal sea-level rise recorded by the previous termRhône deltaic systemnext term (NW Mediterranean)

S. Berné[a, *], G. Joueta[b], M.A. Bassetti[c], B. Dennielou[a] and M. Taviani[d]

[a]Ifremer, Géosciences Marines, BP 70, 29280 Plouzané, France
[b]UMR-CNRS 6538, Domaines Océaniques, IUEM, Plouzané, France
[c]Université de Perpignan, Laboratoire Images, 52 Ave P. Alduy, 66860 Perpignan Cedex, France
[d]ISMAR-CNR, Via Gobetti 101, 40129, Bologna, Italy

*: Corresponding author : S. Berné, email address : serge.berne@univ-perp.fr

Abstract:

A unique late Glacial–Preboreal record of changes in sea-level and sediment fluxes originating from the Alps is recorded in the Rhône subaqueous delta in the Western Mediterranean Sea. The compilation of detailed bathymetric charts, together with high-resolution seismic profiles and long cores, reveals the detailed architecture of several sediment lobes, related to periods of decreased sea-level rise and/or increased sediment flux. They are situated along the retreat path of the Rhône distributaries, from the shelf edge and canyon heads up to the modern coastline. They form transgressive backstepping parasequences across the shelf, the late Holocene (highstand) deltas being confined to the inner shelf. The most prominent feature is an elongated paleo-shoreface/deltaic system, with an uppermost sandy fraction remolded into subaqueous dunes. A long piston core into the bottomsets of this prograding unit allows precise dating of this ancient deltaic system. In seismic data, it displays aggradation, starting at ~ 15 cal kyr BP, followed by progradation initiated during the first phase of the Younger Dryas, a period of reduced sea-level rise or stillstand. The delta kept pace with resumed sea-level rise during the Preboreal (which is estimated at about 1 cm/yr), as a result of increased sediment supply from the Alps (melting of glaciers and more humid climate "flushing" the sediment down to the sea). Abandonment of the delta occurred around 10,500 cal yr BP, that is to say about 1,000 yr after the end of the Younger Dryas, probably because decreased sediment flux.

Keywords: Sea-level; Deglacial; Younger Dryas; delta; Western Mediterranean Sea

1. Introduction and background

The direct record of sea-level rise for the last deglacial period has been mainly determined from the position of reef-crest *Acropora* corals living at less than 5 m of water depth (Fairbanks, 1989; Bard et al., 1996). Another way to explore this record is to study the retreat path of fluvial systems. Estuaries and deltas are depocenters that may leave on the shelf large quantities of sediments from their landward migration. The amount of preserved deposits is thought to be mainly a function of the energy of coastal and marine processes, of the amount of sediment supplied, and of the rate of relative sea-level rise. For instance, some authors have estimated the last deglacial sea-level rise by dating continental fragments of coastal sedimentary environments deposited along the retreat path of large rivers on the Sunda Shelf (Hannebuth et al., 2000). In areas where sediment supply is high, prograding transgressive deposits (parasequences in the sense of Van Wagoner et al. (1990)) formed during periods of deceleration of sea-level rise. First described in the stratigraphic record, they have also been identified in Quaternary sedimentary environments (Anderson and Thomas, 1991). However, autogenic processes (such as the change of sediment flux due to increased rainfall, or the avulsion of deltaic systems) may mimic parasequences induced by sea-level forcing, as discussed by Harris (1999).
In the Gulf of Lions (Fig. 1), Aloïsi et al. (1975) were the first who recognized the architecture of sediment bodies linked to the Rhône retreat during the last sea-level rise. Using seismic and core data, they demonstrated that an elongated sediment body, roughly parallel to the bathymetric contour lines, was situated at a water depth of about 50 m. They suggested that this sediment body was Younger Dryas in age, and formed during a sea-level stillstand followed by a slight fall in sea-level. Further investigations more precisely defined the morphology of the subaqueous delta (Tesson et al., 1998) and the shape of some of its constituting sediment bodies (Gensous et al., 1993; Marsset and Bellec, 2002). The compilation of a large set of seismic data allowed Labaune et al. (2005) to propose a synthesis of the architecture of various seismic units composing the transgressive subaqueous Rhône delta, but details of the morphology and chronostratigraphic framework were not available until now.

2. Terminology

2.1. Subaqueous deltas

The term of subaqueous delta employed in this study corresponds to the sediment bulge which formed by accumulation of sediments during the retreat of the Rhône river during the last deglacial sea-level rise and subsequent highstand. It includes remains of various submarine and subaerial depositional environments left by the retreat: delta plain, beach barriers, delta front, prodelta. It does not include the modern wedge-shaped sediment body that extends westward of the Rhône, a subaqueous delta in the sense of Cattaneo et al. (2003), that results from westward alongshore sediment transport.

2.2. Shoreface

The shoreface of many authors is the portion of shallow-marine depositional system that lies between low tide level and the fair-weather wave base, generally situated at 5-15 m below sea-level (Walker and Plint, 1992). The *fair-weather wave base* corresponds to the limit of the zone where sand transport occurs on a day-to-day basis. In our view, this definition is not precise and does not correspond to an easily identified sedimentological boundary. As proposed by Van Wagoner et al. (1990), we will consider the *storm-wave base* as the lower boundary of the shoreface because the shape and structure of shoreface deposits described in this paper likely represent the long-term product of episodic storms.

2.3. Parasequence

Is used in the sense of van Wagoner et al. (1990) as "relatively comformable successions of genetically related beds or bedsets bounded by marine flooding surfaces or their correlative surfaces". They are separated by a marine-flooding surface, across which there is evidence of an abrupt increase in water depth. In transgressive deltaic environments of the stratigraphic record, parasequences form backstepping units that are often attributed to short period (<100 kyr) cycles of relative sea-level changes. From a sedimentary environment point of view, a parasequence includes the shoreface, as previously described, and the foreshore (beach) deposits. In a deltaic setting, it would include the delta plain, beach ridges, delta front an prodelta.

3. General setting

3.1. Structural framework

The Gulf of Lions is a passive margin which formed in response to late Eocene-Oligocene rifting and subsequent drifting of Corsica and Sardinia (see reviews by Guennoc et al. (2000) and Berné and Gorini (2005)). The margin prograded during the Miocene, accommodation space being mainly provided by thermal subsidence due to the cooling of the oceanic crust. On the shelf, Miocene deposits are topped by a major erosional surface formed during the Messinian salinity crisis (Ryan and Cita, 1978). The existence of the Rhône during the Messinian is attested by a deeply incised valley that formed in response to a sea-level fall of about 1,500 m (Clauzon, 1974). Seaward, the incision is easily mapped up to the pre-Messinian shelf edge (Guennoc et al., 2000; Lofi et al., 2005).

3.2. The Quaternary

The thickness of Quaternary deposits (sediments deposited since 1.87 Ma) at the position of the modern Rhône outlet is about 400 m (Debrand-Passard et al., 1984). In fact, some of the sediments that constitute the present Rhône deltaic plain originate from the Durance, a stream that became a tributary of the Rhône only during the last glacial period. Studies of the modern deltaic plain show that it is made of sandy beach ridges, flood plain and lagoonal deposits, dissected by numerous paleo-channels (L'Homer et al., 1981; Arnaud-Fassetta, 1998; Vella, 1999). The position of the early highstand shoreline is about 15 km landward, the Holocene deposits (marine and terrestrial) thickness reaching about 50 m below the delta plain (Vella et al., 2005).

The architecture of the Rhône subaqueous delta is mainly known from seismic surveys that revealed the organization of late Pleistocene/Holocene deposits (Fig. 2). These investigations demonstrate that the transgressive/highstand deposits form a lobate wedge with a maximum thickness at sea of about 50 m (Aloïsi et al., 1975; Aloïsi, 1986). Because of the littoral drift and the general anti-clockwise water circulation in the Gulf of Lions, there is a strong asymmetry in the thickness of these deposits between the eastern and the western sides of the Rhône subaqueous delta, the transgressive/highstand deposits forming an elongated sediment body stretching to the west (Fig. 3). Further west, the littoral prism is also fed by Languedocian and Pyrenean streams such as Herault, Aude, Agly, Tet, but they presently account for less than 10% of the total sediment budget in the Gulf of Lions (Arnaud-Fassetta, 1998).

3.3. Hydrodynamic setting

The water circulation in the Gulf of Lions is mainly driven by the cyclonic Liguro-Provencal or Northern Current (Millot, 1987, 1999). A shallow branch of this current occasionally penetrates over the shelf, whereas the main outer branch permanently flows southwestward along the slope. This latter branch

has a width of about 30-50 km and a thickness of about 300-500 m. The current speed decreases from 30 to 50 cm/s at the surface to a few cm/s at 500 m depth (Durrieu de Madron et al., 1999). On the western Gulf of Lions continental shelf, measurements have been carried out during extreme events (Guillen et al., 2006). They show that during easterly storms, significant wave heights are in excess of 7 m, with period of about 12 s. Corresponding orbital velocities near the bed reach up to 1.2 m/s at 28 m water depth.
The shelf, about 60 km wide in the central part of the Gulf of Lions, narrows to both the east and west. The shelfbreak is located at water depths ranging from 100 to 150 m, depending on the occurrence or not of recent slope failures within the submarine canyons (Berné et al., 2002a).

4. Data and methods

4.1. Bathymetry

The source data mainly consists of 76 sounding charts at the 1/10000 scale (i.e., soundings along a square grid with a 100 m x 100 m spacing) for water depths ranging from 0 to 50 m, and 54 sounding charts at the 1/20000 scale for water depths ranging from 50 to 150 m. The data set covers the entire Gulf of Lions (Fig. 1). These data, acquired in the 70's and 80's by the Hydrographic Service of the French Navy (Service Hydrographique et Océanographique de la Marine, SHOM), were positioned with the Syledis radio-electrical system, giving a horizontal accuracy better than about 10 m. The vertical accuracy of sounding data, after correction from tidal and meteorological effects, is better than 1 m.
Manual interpretation of this large data set (with 1 m-spaced contour lines) was digitized. Geostatistical interpolation and gridding with 50 m spacing allowed creating Digital Terrain Models (DTM) with spacing of 50 and 100 m (Berné et al., 2002a). In addition, some areas were surveyed by Ifremer with SIMRAD EM950 and SIMRAD EM1000 swath bathymetric systems during cruises in 1995, 2002 and 2003. Additional mapping with “Beautemps Beaupré” was carried out by SHOM in 2004, using a Simrad EM1002S swath bathymetric system.

4.2. Geophysical data

During the same cruises, we employed an SIG sparker (200-600 Hz, 700 Joules) for high-resolution sub-bottom studies, with a shoot interval of 1 or 2 s, at a ship speed of ~ 6 knots. Digital data were acquired and processed on board using a Delph 2 system (swell filtering, gain adjustements, etc.). They were post-processed using Ifremer proprietary software. A hull-mounted Chirp sub-bottom profiler, working at a frequency of 2,500 to 5,200 Hz, was also utilized for ultra-high resolution. For all of these cruises, vessel location data were obtained with a Differential Global Positioning System, providing accuracy in the range of few meters.

4.3. Sedimentology data

In total, 28 cores from the Rhone subaqueous delta were collected and examined, but only 5 are presented in this paper. Piston corers, including the giant piston corer “Calypso” of R/V “Marion Dufresne”, were utilized. Cores in muddy areas are of good quality and undisturbed. Because of the shallow water depth of the sites, “stretching” of the cores (Skinner and McCave, 2003) did not occur. Using distinct seismic horizons for evaluating actual core penetration, we found a loss of about 0.5 m at the top of the long (16 m) Calypso core MD992352. The position of a major discontinuity (D350) on seismic profiles correlates well with the actual position of a coarse lag at the bottom of this core, using measured sonic velocities, thus confirming the absence of core deformation. In sandy areas, a vibracorer designed by Rice University was utilized. Well-preserved mollusc and bivalves shells plus calcareous tests from microfauna associations were collected from 5 cores (position in Fig. 3). Radiometric dates of these samples were obtained with accelerator mass spectrometer (AMS) ^{14}C at the Lawrence Livermore National Laboratory (LLNL) and at the Poznan Radiocarbon Laboratory

(PRL). The ages reported herein are delta13C-normalised conventional 14C years. All ages being comprised between 0 and 21,880 yr ^{14}C BP, calendar (i.-e. calibrated) ages were calculated using the Calib 5.0 sofware (Stuiver and Reimer, 1993). For marine material, the Marine04 calibration curve (Hughen et al. 2004) was used with no deviation from the average reservoir age (-408 years). For continental material (namely the organic debris of the St Ferreol prodelta) the Intcal04 calibration curve (Reimer et al., 2004) was used.
Data were incorporated into a Geographic Information System (GIS), allowing easier comparison of various data sets.

5. Results

5.1. Overall architecture of the subaqueous deltaic complex

A general topographic/seismic profile across the continental shelf in the Gulf of Lions illustrates the various morphologies and stacking patterns related to the late Quaternary history of the Rhône system (Fig. 2). From south to north (in the direction of shore retreat during the deglacial sea-level rise), they consist of:

-Prograding sequences (S0 to S5) with internal clinoforms corresponding to Pleistocene forced regressions that formed during 100 kyr glacial cycles (Aloïsi, 1986; Rabineau et al., 2005). Outcropping of the last lowstand shoreface sands ("offshore sands") between 90 and 120 m water depth form a distinct morphology, bounded to the south by a major step that corresponds to the limit between upper shoreface sands and lower shoreface muds. The sea-floor on the outer shelf is characterized by erosional morphology. Remnants of beaches cemented during glacial periods (beach rocks) form several meter high pinnacles (Berné et al., 1998).

-Backstepping units (U300 to U500 in Fig. 2) form the deglacial and highstand Rhône subaqueous delta. The seafloor lithology is dominated by silts and clays, except for an elongated sand body situated at about 45-50 m water depth, that will be described hereafter.

The bathymetric map reveals the main geomorphic features that constitute the Rhône subaqueous delta (Fig. 3). Using the same data set, a slope map was created in order to better visualize slope gradients (Fig. 4).
Several geomorphic features are identified, from south to north:
In the vicinity of the "Petit Rhône" canyon head, very distinct steps at 110-115 m (1 in Figs. 3 and 4) and 98 m (2 and 3 in Figs. 3 and 4) are features observed elsewhere in the Gulf of Lions (Berné et al., 2002a; Jouet et al., 2006). They correspond to periods of decreased sea-level rise during the early deglacial. Further to the west, they have been dated at 18,000-17,000 cal. yr BP (feature 1) and >15,500 cal. yr BP (features 2-3) (Jouet et al., 2006).
The main retreat path of the Rhône (4 in Figs. 3 and 4) appears to be clearly visible from its canyon head (the "Petit Rhône" canyon head) to the south up to the –60 m contour line to the north. Between the –75 m and –65 m contour lines, preserved channel/levee facies can be observed, suggesting that the sea-level rise was fast enough to limit erosion by wave action. This facies disappears landward at about –65 m, where it is buried by muds from more proximal prograding units. Other, similar but less distinct features (4w1, 4w2 and 4e) are attributed to other distributaries of a Lowstand Rhône deltaic system. It is worth noting that 4w1 connects to the Marti canyon head, indicating that the "Petit Rhône" canyon was not the only sink for sediments from the Rhône during the last glacial cycle.
On the inner shelf, 6 major elongated or semi-circular sediment bodies can be identified, based on increased gradient in seafloor slope (5 to 10 in Figs. 3 and 4). These features are inferred to correspond to the remains of past deltaic lobes. The most distinguishable feature is located in the western part of the subaqueous delta, between the –55 and –35 m contour lines (Lobe 5 in Figs. 3 and 4). It roughly corresponds to the position of the sand body that was initially described by Aloïsi et al. (1975). Other, more recent features (Lobes 6 to 10 in Figs. 3 and 4) are also preserved. The upper 5.60 m of Lobe 6 were sampled by core BMKS21 (position in Fig. 3). It consists of clayey silt which yield ages, from bottom to top, between 2,500 and 2,050 yr cal. BP (Table 1). These dates are compatible with the age of the St Ferreol deltaic lobe mapped onshore (2,000-4,000 yr cal BP (Vella et al., 2005)) and Lobe 6 is likely the marine (prodeltaic) equivalent to the St Ferreol delta. Similarly, the NW-SE bathymetric step running from Pointe de l'Espiguette to the -25 m contour line (Lobe 7 in Figs.

3 and 4) may correspond to a former Peccais deltaic lobe, and/or could be the submarine prolongation of a sand spit formed by modern processes (Sabatier et al., 2006). The Lobe 8 in Fig. 3 is the marine component of the “Bras de Fer” system recognized onshore (Arnaud-Fassetta, 1998), that formed during the Little Ice Age, whereas the Lobe (9) certainly corresponds to the remains of the “Peygoulier” lobe, that formed after the avulsion of the Bras de Fer during the major floods of 1709-1712, and was active until it was diverted toward the modern “Roustan” delta lobe (feature (10) in Figs. 3 and 4) during the 20 th century (Arnaud-Fassetta, 1998). Comparison of bathymetric data sets acquired since 1842 show that these two lobes are presently experiencing erosion (Sabatier et al., 2006).

5.2. The Early Rhône Deltaic Complex (ERDC)

Besides the “offshore sands” that blanket the entire outer continental shelf, beyond about 90 m water depth, the largest sand body in the Gulf of Lions is the one labeled as “Lobe 5” in Figures 3 and 4. In fact, this sand body represents the topset region of a prograding system corresponding to unit U400 of Figure 2. We will successively examine its morphology, lithology, and internal structure.

5.2.1- Detailed morphology and surficial lithology of the Early Rhône Deltaic Complex

Part of the ERDC was mapped with swath bathymetric systems that reveal two types of bedforms at the top of the sand body (Fig. 5):
Longitudinal bedforms, oriented NW-SE. They are less than 3 m high, with a spacing of about 600 m. In fact, the orientation of these features changes from the west to the east, the overall shape being curvilinear. To the north, they are buried under unit U500 (that corresponds to the more recent St Ferreol deltaic lobe), and therefore considered to be fossil. They are very similar in shape and orientation to the beach ridges described in the recent St Ferreol deltaic lobe (L'Homer et al., 1981) and are therefore interpreted as preserved beach ridges.
Transverse dunes, up to 4 m high, with a spacing of about 500 m. The dunes have a main axis oriented in a N-S direction; however, they often display a polygonal character that could be due to varying directions of sediment transport under different wind-driven circulation regimes.

When compared to the sediment distribution in the area (Fig. 1), it appears that the occurrence of both longitudinal and transverse bedforms corresponds to the availability of sandy sediment. It can be noted that the water depth of dune distribution does not strictly follows the bathymetric contour lines: the lower limit of dunes is around -60 m to the east, whereas it is only 45 m to the west.

5.2.2- Seismic facies and architecture

In cross section, the ERDC displays clinoforms (seismic unit U400 of Fig. 2) topped by a zone remolded by dunes. U400 is better seen on profiles with less vertical exaggeration (Line Bas1-38, Fig. 6). It forms a seismic sequence, up to 30 m thick, that pinches out seaward at about 90 m water depth. Landward, this seismic unit is overlain by late transgressive or highstand deposits of the Rhône subaqueous delta (U500 and other seismic units, see Labaune et al. (2005) for detailed geometrical description). Its internal seismic geometry corresponds to large-scale (10-20 m) tangential clinoforms, truncated at their top by a wavy surface, downlapping on unit U350. The maximum angle of dip of the clinoforms is between 0.5 and 1°, that is to say about the same as the muddy clinoforms of the Adriatic shelf (Cattaneo et al., 2004), but less than the very sandy clinoforms of the Gulf of Lions outer continental shelf where angles are as high as 5° (Berné et al., 1998). In detail, chirp seismic profiles show that the upper erosion surface that overlies U400 is a distal equivalent to D500 (that separates U400 from U500 in the landward direction), and sometimes separates the clinoforms of U400 from an upper thin unit, not distinguished on sparker profiles. Within the upper part of the clinoforms, there is also a distinct change in seismic facies (Fig. 7), with:

An upper, chaotic facies (Fig. 7-1), with numerous cut and fill structures, typical of deltaic environments (Berné et al., 2002b; Abdulah et al., 2004; Roberts et al., 2004; Correggiari et al., 2005).

A lower clinoform facies (Fig. 7-2) with continous and parallel to sub-parallel reflections, typical of prodeltaic environments (Cattaneo et al., 2004; Trincardi et al., 2004).

Medium-scale (1-3 m) clinoforms with an apparent angle of dip in the Northern direction are stacked in the upper part of unit U400 (close-up view 1 in Fig.2). This implies that some sediment transport in a landward or shore-parallel direction occurred at the end of the deposition of U400 (washover or alongshore transport in a lagoon isolated by a barrier island).
The lower boundary of U400 (D400) is not a pronounced reflector, and was therefore omitted in earlier interpretation (Labaune et al., 2005). It corresponds, however, to a distinct downlap surface, sometimes underlined by the presence of shallow gases underneath (Fig. 11). It can be mapped regionally on strike seismic profiles (Fig. 12).

5.2.3. Sedimentary facies and environments, chronostratigraphy

Piston and vibracores where collected from the topset, foreset and bottomset regions of the ERDC in order to characterize lithologies, determine sedimentary environments from primary structures and mollusc assemblages, and obtain chronostratigraphic constraints through radiocarbon dating.

Lithology of the topset area (sand dune/sand ridge area)
All the 16 sediment cores available from the topset region are fairly short, due to difficulty of core penetration and recovery in sandy material. Therefore, the cores did not reach the underlying deltaic facies that are observed on chirp seismic profiles. Most of the cores, such as core BMVK06 shown in Fig. 8, or core BMKS16 positioned in Fig. 5 exhibit a distinct coarsening-upward pattern, with, from bottom to top, fine to medium sand beds alternating with silty intervals, progressively or abruptly passing to massive fine to medium sands (up to 1.50 m thick). They are topped by coarse bed(s) 5-30 cm thick, with shells, shell debris and some pebbles and cobbles. Most of individual sand beds observed in the zone of alternating sand and silt exhibit a fining-upward pattern. The erosion surface observed at the top of U400 on seismic profiles is consistent with several cores containing a very coarse lag including shell and shell fragments originating from shoreface and very shallow water environments. At the top of most of the cores, especially in vibracores where the upper beds are better preserved, unconsolidated silty clay, up to 80 cm thick, is observed, suggesting that the underlying dunes are not in equilibrium with the hydrodynamic regime, at least during periods of fair weather. The coarsest samples were found at the eastern end of the ERDC, with a zone blanketed by cobbles and pebbles (core STKS 25, Fig. 9), indicative of the vicinity of a fluvial system. It is worth noting that along the modern Rhône, pebbles are not found south of Arles, about 50 km upstream of the present river outlet (Vella, Pers. Comm.). This implies that the capacity of bedload transport of the Rhône was much higher at the time of deposition of the ERDC.

Lithology of the foreset/bottomset area (core MD992352)
The longest core from the foreset/bottomset region was obtained with the “Calypso” piston corer of “Marion Dufresne”. Core MD992352 is 15.40 m long and provides the most expanded record of seismic units U400 and U350 (Fig. 8 and Table 1).
At its base (1538-1529 cm), this core displays a very coarse and shell-bearing horizon with flat cobbles (up to 2 cm in diameter) interpreted as a ravinement surface. This strata likely corresponds to seismic surface D350. The skeletal assemblage above that surface is a muddy-shell hash that contains mollusc shells of diverse ages sourced from various littoral and sublittoral environments. In particular worn bioclasts belonging to the bivalve Mytilus sp. (cf galloprovincialis) dated at ~ 15,000 cal yr BP, together with Chamelea gallina and the gastropod Nassarius reticulatus, represent the shallowest (therefore oldest) components included in such assemblage and interpreted as a very shallow-water environment (0-2 m water depth) cannibalized during the transgression. Other components in this same hash include the boreo-celtic guest Mya truncata, and holoplanktic molluscs such as thecosomatous pteropods (Limacina sp.).
Above the ravinement surface, the core displays a long interval of clayey silts, interrupted by mm-thick laminae to cm-thick beds of sandy silt or fine sand, indicative of a lower shoreface/prodeltaic environment. Molluscs representative of muddy, prodeltaic settings, such as Turritella communis and Corbula gibba, confirm this interpretation.
Between 102 and 140 cm, a shell bed and shell hash in a matrix of fine sand is observed, and this likely corresponds to seismic surface D500 (if we consider that about 0.5 m of upper fine sediments were lost during the coring operation). The skeletal assemblage is very diverse and includes molluscs, bryozoans and serpulids from different shelf environments. This bed is interpreted as documenting a phase on intense sea-floor winnowing (condensed interval).

The upper 102 cm is a bioturbated, beige, silty clay with some shells and shell debris. The occurrence of Parvicardium minimum, Acanthocardia echinata, Nassarius pygmaeus and especially Corbula gibba, documents a modern prevalently muddy shelf environment with episodic reworking of sediment (e.g., Cabioch, 1968; Di Geronimo and Robba, 1989; Taviani et al., 1998). Pteropods such as Cavolinia inflexa indicate a pelagic contribution.
The ages of dated material are reported in Table 1. Except for one sample composed of mixed material (benthic foraminifera, bivalves, gastropods and ostracods), the results do not show any age inversion within the 1-sigma error interval. From these results, an age model was established for the interval situated between the two erosion surfaces (D350, the ravinement surface situated at the bottom of the core, D500, the upper erosion surface) (Fig. 10).

6. Discussion

6.1. What is the ERDC and when did it form ?

The elongated geometry and internal seismic architecture of the ERDC present similarities with that of the *infralittoral prograding wedges* described along the Spanish Mediterranean coast (Hernandez-Molina et al., 2000). These sand bodies have been interpreted by these authors as the product of downwelling storm currents and are therefore modern sand bodies in equilibrium with present oceanographic processes. In contrast, the age of the bottomsets of the ERDC demonstrates that it is a relict feature, even though modern processes might episodically reactivate its surface during extreme events. We have seen that the sandy upper part of the ERDC likely corresponds to the remains of a shoreline that deposited during a slow down of the deglacial sea-level rise. It is difficult to date precisely beach deposits, that incorporate material of very different origin and age. Therefore, we used the dates from the coeval deposits of the lower shoreface/prodelta domain. Using the ultra-high resolution seismic profiles, we used clinoforms as time-lines, in order to propagate the radiocarbon age model from the bottomset region (core MD992352) to the foreset/topeset area.
Each clinoform on the seismic profile (labeled 1 to 11 in Figure 11) is a time-line which can be dated at the intercept with the position of core MD992352 (Table 2). If we plot these time lines from the position of the core in a landward direction, we may infer the age of the corresponding sandy foresets, as well as the age of the transition zone between the deltaic/prodeltaic seismic facies, that approximates sea-level position. This technique indicates that deposition of the ERDC began, in our study area, around 15,000 yr cal BP, above the coarse lag of the ravinement surface (D350), and stopped around 10,500 yr cal BP. We cannot exclude that marine sedimentation began earlier, and in that case older ravinement surfaces would be preserved below D350, but the age and nature of Unit 300 seen in Fig. 6 are unknown as we have not been able to collect any core from this interval. This 15,000-10,500 yr cal BP time-frame encompasses the end of the Bølling-Allerød, the Younger Dryas and the Preboreal. Maximum sedimentation at the position of our core occurred between 11,500 and 10,500 cal yr BP, during the Preboreal. Seismic surface D400, identified as a downlap surface, has an interpolated age of about 12,049±62 cal yr BP (Fig. 10). This age corresponds to the beginning of the Younger Dryas, a time of reduced sea-level rise (Fairbanks, 1989) or even still-stand when the ERDC shifted from aggradation to progradation. The end of deposition of the EDRC does not coincide with the termination of the Younger Dryas, but lasted until ~ 10,500 cal yr BP, about 1,000 years after the end of this cold event.
The erosional surface observed at the top of the ERDC (D500) is younger than 10,500 cal yr BP. Therefore, it can not be attributed to a sea-level fall during the Younger Dryas, as hypothesized by Aloïsi (1986). On the contrary, it might correspond to a phase of starvation during a phase of increased sea-level rise. It is an equivalent to the transgressive condensed interval described on the outer shelf (Bassetti et al., 2006).

6.2. Relative sea-level changes and shoreline progradation

A way to evaluate sea-level position from our seismic data is to measure the depth of the transition between the distinct deltaic and prodeltaic seismic facies shown in Fig. 7. This transition point, which roughly represents the *shoreline trajectory* (as described by Helland-Hansen and Martinsen (1996) and discussed by Hampson and Storms (2003)), has been plotted on chirp seismic profiles (marked

by X symbols in Fig. 11). This boundary between seismic facies is not extremely precise, but certainly has a depth error bar similar to that of *Acropora* used in coral reef studies (i.e., about 5 m). Furthermore, the migration of this transition zone, as it can be tracked across clinoforms, is a good indicator of the *rate* of sea-level change. Our results are not corrected for any glacio- or hydro-isostatic effect, and therefore should be considered as *relative* sea-levels. Estimates of hydro-isostatic effect at the shelf edge is in the order of 20 m for the last 20kyr (Jouet et al., in press). However, numerical modeling of mantle rheology suggests that, in our study area and for the considered period, the glacio-isostatic contribution roughly balanced the hydro-isostatic effect (Lambeck and Bard, 2000). In all of our results, we do not take into account the depth of the brinkpoint (-47 m) observed on bathymetric and seismic data because we do not know whether it corresponds to the top of a paleo-delta front or to a preserved coastal dune.

The depth of the transition zone between deltaic and prodeltaic seismic facies can be measured on Clinoforms 6 to 11, with corresponding ages comprised between ~ 11,100 and ~ 10,600 cal yr BP (Table 2), that is to say the end of the Preboreal chronozone. The validity of our method is confirmed by the age of the bottom of core BMVK06 from the topset region (10,665-10,899 cal yr BP, Table 1), compared to the age of the nearest clinoform (clinoform 11, dated at 10,595±161 cal yr BP, Table 2). According to our data, relative sea-level rose from about -55 m to about -50m during this interval, at an average rate of 1.02 cm/yr. More precisely, the rate of sea-level rise was on the order of 0.3-0.6 cm/yr between ~ 11,100 and 10,900 cal yr BP, then about 1.2 cm/yr from ~ 10,900 to 10,600 cal yr BP.

Shoreline advance in our study area can also be estimated from the intercept between the top of the clinoforms and the sea-floor in a shore-normal direction. This measurement is only possible between about 11,000 cal yr BP (Clinoform 8) and the brink point. It decreases from about 15 m/yr around 11,000 cal yr BP to 2.4 m/yr around 10,600 cal yr BP. Without any avulsion or change in sediment flux, this decrease could simply be explained by an increased rate of sea-level rise creating more accommodation.

6.3. Sequence stratigraphic interpretation of the ERDC

In a sequence stratigraphic framework, the ERDC corresponds to a *transgressive parasequence* bounded by *flooding surfaces* (Fig. 13) in the sense of Van Wagoner et al. (1990). Our precise chronology allows us to link key surfaces to phases of (relative) sea-level change:

The basal bounding surface corresponds to sea ingression during the Bølling-Allerød, and is therefore a true flooding surface.

The downlap surface (D400) that mimics a maximum flooding surface represents the end of this rapid sea-level rise. It formed during the first phase (around 12,000 cal yr BP) of the Younger Dryas stillstand or decelerating sea-level rise. It is a *surface of maximum transgression* in the sense of Helland-Hansen and Martinsen (1996).

The upper boundary (surface D500) is also a flooding surface, but it formed with a delay of about 1,000 yr with respect to the resumed sea-level rise. This implies that it can no more be considered as an erosion surface formed by stillstand or sea-level fall at the end of the Younger Dryas (Aloïsi et al., 1975; Gensous and Tesson, 2003; Labaune et al., 2005).

The sand that constitutes the upper part of the ERDC originates from an ancient shoreline/delta front, with the possible position of a Rhône outlet at the position of core KSTR 25 where cobbles and pebbles are found. Longitudinal bedforms parallel to this paleo-shoreline are relict feature, their northern termination being buried by the Holocene muds. It is not clear whether transverse dunes from the same area are fossil or still subject to episodic migration during high-energy events, such as the outer shelf dunes described by Bassetti et al. (2006).

The bathymetric position of the ERDC and the chronology of its deposition is similar to other transgressive parasequences described elsewhere. For instance, the extensively studied Northern Gulf of Mexico margin displays several transgressive backstepping deltas that formed during the same time period (Anderson et al., 2004). In particular, the Colorado river formed, between 14,000 and 11,000 yr BP, a backstepped delta at -45 m (Abdulah et al., 2004) that corresponds, in time and position, to the ERDC. In the Adriatic, several backstepped units are also preserved in similar stratigraphic and bathymetric positions (Trincardi et al., 1996; Cattaneo and Trincardi, 1999; Asioli et al., 2001; Cattaneo et al., 2003).

6.4. Processes controlling the late progradation and abandonment of the ERDC

Changes in the rate of relative sea-level rise (that control accommodation) and/or changes in the amount of sediment supply may explain the evolution of the ERDC, and its abandonment at ~ 10,500 cal yr B.P, that represents a delay of ~1,000 yr following the Younger Dryas cold interval.

6.4.1. Sea-level

Positions of sea-level inferred from our data correspond very well with that from global studies (Fig. 14), even though they are uncorrected sea-levels. We note in Table 2 an increase in the slope of the shoreline trajectory that suggests an increase in the rate of sea-level rise at the end of the progradation phase of the ERDC. However, this observation is based on only 2 measurements, and, for this 11,100-10,600 cal yr BP time-period, there is a large consensus about a constant sea-level rise. For instance, Lambeck et al. (2002) propose a constant global sea-level rise of 1.52 cm/yr for the Post Younger Dryas- 8,500 cal yr BP time window. Similarly, Camoin et al. (2004) propose for the Indian Ocean a minimum value of 1.16 cm/yr for the 11,600–9,640 cal yr BP time window, that can be compared to the 1.2 cm/yr measured in the Gulf of Lions. Some authors have argued that, besides MWP1A and MWP1B, other Melt Water Pulses occurred during the last deglacial sea-level rise (Liu et al., 2004). However, even if real, the chronology of these events, especially their so-called MWP 1c, does not correspond to our period of possible increased sea-level rise.

6.5. Sediment flux

Sequence stratigraphers have shown that shoreline progradation (regression) may occur in a context of sea-level rise, provided that sediment flux is sufficient to fill the available space (Posamentier et al., 1992). The ~ 1,000 yr delay between the end of the Younger Dryas and the period of delta abandonment may be explained by a phase of increased sediment flux during the beginning of the Preboreal. This hypothesis is supported by studies in the catchment area of the Rhône, for instance in Lake Lautrey of Jura where Younger Dryas is characterized by very low sedimentation rate (about 0.2 mm/yr), whereas the warmer Preboreal has a sedimentation rate about 6 times higher (Magny et al., 2006). It is very likely that melting of Alpine glaciers due to Preboreal warming, and increased rainfall during the same period, favored the supply of a huge amount of sediment to the sea, following the dry and cold Younger Dryas. As to the abandonment of the ERDC at 10,500 cal yr BP, it could be due to a purely autocyclic process, the delta being switched further west, as suggested by the WNW-ESE trend of the ERDC and the progressive shallowing of the sand/silt transition in the WNW direction. A climatic control is however likely, as a phase of aridification is observed all around the Western Meditteranean Sea at the same time (Magny et al., 2002).

In summary, we consider that the initiation and growth of the ERDC was mainly controlled by a decreased rate of sea-level rise. In contrast, the ERDC was able to keep pace with renewed increase of sea-level rise after the Younger Dryas mainly because increasing sediment flux.

In the future, it will be interesting to explore the relative effect of changes in temperature and rainfall on the amount of sediment supplied to the ERDC, and more generally to the Rhône deltaic system. 3D stratigraphic modeling constrained by seismic geometries and ^{14}C dates will permit to test these hypothesis, and to quantify the relative impact of sediment flux and sea-level changes on sequence architecture.

Conclusions

The morphology and internal architecture of the Rhône subaqueous delta exhibit the imprint of deglacial sea-level rise strongly influenced by changes in sediment supply. Early phases in the rise are evidenced by 2 morphological steps at 110-115 and 98 m water depth. The rapid sea-level rise during Meltwater Pulse 1A resulted in the retreat of the Rhône along a N-S path that is well preserved in the present seafloor morphology, in the form of a channel-levee system. The ERDC was deposited between about 15,000 and 10,500 cal yr BP, forming a major transgressive parasequence on the middle/inner shelf. This complex consists in a lower retrograding/aggrading unit, that formed during a period of rapid sea-level rise (15,000 to 12,000 cal yr BP), and an upper prograding unit initiated during the slow sea-level rise of the Younger Dryas. However, due to increased sediment flux during the Preboreal, progradation was maintained until about 10,500 cal yr BP, about 1,000 yr following the

end of the Younger Dryas, at a time when the rate of sea-level rise was in the order of 1 cm/yr. The abandonment of the deltaic complex at 10,500 cal yr BP is attributed to a decrease in sediment supply, rather than to an increased rate of sea-level rise. The origin of this sediment starvation can be linked to a phase of aridity and/or to a shift of the Rhône to the West.
Despite the general idea that the last deglacial sea-level rise was too fast for allowing deposition of large sediment bodies on the shelf, our study demonstrates that most of the sediment accumulated on the inner and mid shelf off the Rhône corresponds to transgressive deposits, late Holocene sediments being accumulated along the coastal zone.

Acknowledgements

This research was supported by the European Community through the Eurodelta (contract EVK3-CT-2001-20001) and Eurostrataform (contract EVK3-2001-00200) projects. The Beachmed cruise was co-funded by the Interreg Medocc project, coordinated in France by Conseil Général de l'Hérault, and by Ifremer. Additional support came from Ifremer, "Region Languedoc-Roussillon" and the French Agence Nationale de la Recherche (Sesame project, contract NT05-3-42040). The French Hydrographic Service (SHOM) gave access to sounding charts, that were interpreted by Daniel Carré. Special thanks are due to Yann Stephan and Gwladys Theuillon who gave access to swath bathymetric data acquired in 2004 with "Beautemps Beaupré", in the framework of the "Calimero project" (convention 8D/003 between SHOM and Ifremer) as well as Xavier Lurton at Ifremer. Captains and crews, as well as the scientific parties of "Marion Dufresne", "Le Suroît" and "L'Europe" are thanked for their participation during cruises "Images 5", "Basar 1 and 2", "Calmar 99", "Marion", "Strataform", GMO 2 (thanks to N. Sultan), and "Beachmed" (thanks to C. Satra). Special thanks are due to N. Thouveny (Cerege) and Y. Balut (IPEV) support during the Images 5 cruise. Colleagues at Ifremer and Genavir (Anne-Sophie Alix, Ronan Apprioual, Daniel Carré, Bernard Dennielou, Fabienne Duval, Gilbert Floch, Nelly Frumholtz, René Kerbrat, Eliane Le Drezen, Estelle Leroux, Laetitia Morvan, Alain Normand, Christian Prud'homme, Delphine Pierre, Catherine Satra, Samuel Toucan), are warmly thanked for their assistance in the various phases of the project. Jean Claude Aloïsi (formerly at University of Perpignan) was at the origin of most of the investigations presented here. Lively discussions with Antonio Cattaneo (Ifremer) about the semantics of transgressive deposits helped improving this manuscript. We are indebted to the two reviewers (Fabio Trincardi, Istituto di Scienze Marina, CNR Bologna and J.P. Walsh, East Carolina University), as well as Marine Geology Editor David Piper, for their comments and suggestions that greatly improved the manuscript. This is IGM scientific contribution n. 1524. This work is dedicated to Daniel Carré and Christian Prud'homme, who passed away recently.

References

Abdulah, K.C., Anderson, J.B., Snow, J.N., Holford-Jack, L., 2004. The Late Quaternary Brazos and Colorado deltas, offshore Texas, USA- Their evolution and the factors that controleld their deposition. In: J.B. Anderson and R.H. Fillon (Editors), Late Quaternary Stratigraphic evolution of the northern Gulf of Mexico margin. SEPM (Society for Sedimentary Geology) Special Publication 79, Tulsa, pp. 237-269.

Aloïsi, J.C., Monaco, A., Thommeret, J., Thommeret, Y., 1975. Evolution paléogéographique du plateau continental languedocien dans le cadre du Golfe du Lion. Analyse comparée des données sismiques, sédimentologiques et radiométriques concernant le Quaternaire récent. Revue de Géologie Dynamique et de Géographie Physique, 17, 13-22.

Aloïsi, J.C., 1986. Sur un modèle de sédimentation deltaïque: contribution à la connaissance des marges passives. Unpublished Doctoral Thesis, University of Perpignan, 162 p.

Anderson, J.B., Thomas, M.A., 1991. Marine ice-sheet decoupling as a mechanism for rapid, episodic sea-level change: the record of such events and their influence on sedimentation. Sedimentary Geology, 70, 87-104.

Anderson, J.B., Rodriguez, A., Abdulah, K.C., Fillon, R.H., Banfield, L.A., McKeown, H.A.Wellner, J.S., 2004. Late Quaternary Stratigraphic evolution of the northern Gulf of Mexico margin: a synthesis. In: J.B. Anderson and R.H. Fillon (Editors), Late Quaternary Stratigraphic evolution

of the northern Gulf of Mexico margin. SEPM (Society for Sedimentary Geology), Tulsa, pp. 1-23.
Arnaud-Fassetta, G., 1998. Dynamiques fluviales holocènes dans le delta du Rhône. PhD Thesis, Université de Provence, Aix en Provence, 329 pp.
Asioli, A., Trincardi, F., Lowe, J.J., Ariztegui, D., Langone, L., Oldfield, F., 2001. Sub-millennial scale climatic oscillations in the central Adriatic during the Lateglacial: palaeoceanographic implications. Quaternary Science Reviews, 20, 1201-1221.
Bard, E., Hamelin, B., Arnold, M., Montaggioni, L., Cabioch, G., Faure, G., Rougerie, F., 1996. Deglacial sea-level record from Tahiti corals and the timing of global meltwater discharge. Nature, 382, 241-244.
Bassetti, M.A., Jouet, G., Dufois, F., Berné, S., Rabineau, M., Taviani, M., 2006. De-glacial sedimentary processes and deposits in the outer continental shelf of the Gulf of Lions (western Mediterranean). Marine Geology, 234, 93-109.
Berné, S., Lericolais, G., Marsset, T., Bourillet, J.F., de Batist, M., 1998. Erosional shelf sand ridges and lowstand shorefaces: examples from tide and wave dominated environments of France. Journal of Sedimentary Research, 68, 540-555.
Berné, S., Carré, D., Loubrieu, B., Mazé, J.P., Normand, A., 2001. Carte morpho-bathymétrique du Golfe du Lion. Ifremer, Brest.
Berné, S., Satra, C., Aloïsi, J.C., Baztan, J., Dennielou, B., Droz, L., Dos Reis, A.T., Lofi, J., Méar, Y., Rabineau, M., 2002a. Carte morpho-bathymétrique du Golfe du Lion, notice explicative, Ifremer, Brest.
Berné, S., Vagner, P., Guichard, F., Lericolais, G., Liu, Z., Trentesaux, A., Yin, P., Yi, H.I., 2002b. Pleistocene forced regressions and tidal sand ridges in the East China Sea. Marine Geology, 188, 293-315.
Berné, S., Rabineau, M., Flores, J.A., Sierro, F.J., 2004. The impact of Quaternary Global Changes on Strata Formation. Exploration of the shelf edge in the Northwest Mediterranean Sea. Oceanography, 17, 92-103.
Berné, S., Gorini, C., 2005. The Gulf of Lions: An overview of recent studies within the French 'Margins' programme. Marine and Petroleum Geology, 22, 691-693.
Camoin, G.F., Montaggioni, L.F., Braithwaite, C.J.R., 2004. Late glacial to post glacial sea levels in the Western Indian Ocean. Marine Geology, 206, 119-146.
Cabioch, L., 1968. Contribution à la connaissance des peuplements benthiques de la Manche occidentale. Cahiers de Biologie Marine 9, 493-720.
Cattaneo, A., Trincardi, F., 1999. The Late-Quaternary transgressive record in the Adriatic Epicontinental Sea: Basin widening and facies partitioning. In: K.M. Bergman and J.W. Snedden (Editors), Isolated Shallow Marine Sand Bodies: Sequence Stratigraphic Analysis and Sedimentological Interpretation. SEPM Special Publication, Tulsa.
Cattaneo, A., Correggiari, A., Langone, L., Trincardi, F., 2003. The late-Holocene Gargano subaqueous delta, Adriatic shelf: Sediment pathways and supply fluctuations. Marine Geology, 193, 61-91.
Cattaneo, A., Trincardi, F., Langone, L., Asioli, A., Puig, P., 2004. Clinoform generation on Mediterranean margins. Oceanography, 17, 105-117.
Clauzon, G., 1974. L'hypothèse eustatique et le creusement prépliocène de la vallée du Rhône. Annales de Géographie, 456, 129-140.
Correggiari, A., Cattaneo, A., Trincardi, F., 2005. The modern Po Delta system: Lobe switching and asymmetric prodelta growth. Marine Geology, 222-223, 49-74.
Debrand-Passard, S., Courbouleix, S., Lienhardt, M.J., 1984. Synthèse géologique du Sud-Est de la France, 125. Bureau de Recherches Géologiques et Minières, Orléans, 615 pp.
Di Geronimo, I., Robba, E., 1989. The structure of benthic communities in relation to basin stability. In: A. Boriani, M. Bonafede, G.B. Piccardo and G.B. Vai (Editors), The Lithosphere in Italy, Atti del Convegno Lincei 80, Accademia Nazionale dei Lincei, pp. 341-352.
Durrieu de Madron, X., Radakovitch, O., Heussner, S., Loye-Pilot, M.D., Monaco, A., 1999. Role of the climatological and current variability on shelf-slope exchanges of particulate matter: Evidence from the Rhone continental margin (NW Mediterranean). Deep Sea Research Part I: Oceanographic Research Papers, 46, 1513-1538.
Fairbanks, R.G., 1989. A 17,00-year glacio-eustatic sea-level record: influence of glacial melting rates on the Younger Dryas event and deep-ocean circulation. Nature, 342, 637-642.
Gensous, B., Williamson, D., Tesson, M., 1993. Late-Quaternary transgressive and highstand deposits of a deltaic shelf (Rhône delta, France). In: H.W. Posamentier, C.P. Summerhayes,

B.A. Haq and G.P. Allen (Editors), Sequence stratigraphy and facies associations. International Association of Sedimentologists Spec. Pub. 18, Blackwell, Oxford, pp. 197-212.
Gensous, B., Tesson, M., 2003. L'analyse des dépôts postglaciaires et son application à l'étud des séquences de dépôt du Quaternaire terminal sur la plate-forme au large du Rhône (golfe du Lion). Bulletin de la Société Géologique de France, 174, 401-419.
Guennoc, P., Gorini, C., Mauffret, A., 2000. Histoire géologique du Golfe du Lion et cartographie du rift oligo-aquitanien et de la surface messinienne. Géologie de la France, 3, 67-97.
Guillen, J., Bourrin, F., Palanques, A., Durrieu de Madron, X., Puig, P., Buscail, R., 2006. Sediment dynamics during wet and dry storm events on the Tet inner shelf (SW Gulf of Lions). Marine Geology, 234, 129-142.
Hampson, G.J., Storms, J.E.A., 2003. Geomorphological and sequence stratigraphic variability in wave-dominated, shoreface-shelf parasequences. Sedimentology, 50, 667-701.
Hannebuth, T.J.J., Statteger, K., Grootes, P.M., 2000. Rapid flooding of the Sunda Shelf- A late-glacial sea-level record. Science, 288, 1033-1035.
Harris, P.T., 1999. Sequence architecture during the Holocene transgression: an example from the Great Barrier Reef shelf, Australia-comment. Sedimentary Geology, 125, 235-239.
Helland-Hansen, W., Martinsen, O.J., 1996. Shoreline trajectories and sequences: description of variable depositional-dip scenarios. Journal of Sedimentary Research, 66, 670-688.
Hughen, K.A. et al., 2004. Marine04 Marine radiocarbon age calibration, 26 - 0 ka BP. Radiocarbon, 46, 1059-1086.
Jouet, G., Berné, S., Rabineau, M., Bassetti, M.A., Bernier, P., Dennielou, B., 2006. Shoreface migrations at the shelf edge and sea-level changes around the Last Glacial Maximum (Gulf of Lions, NW Mediterranean Sea). Marine Geology, 234, 21-42.
Jouet, G., Hutton, E.W.H., Syvitski, J.P.M., Berné, S., in press. Response to loading and subsidence of the Rhône deltaic margin during the Last Climatic Cycle. Computers & Geosciences.
L'Homer, A., Bazile, F., Thommeret, J., Thommeret, Y., 1981. Principales étapes de l'édification du delta du Rhône de 7000 B.P. à nos jours ; variations du niveau marin. Oceanis, 7, 389-408.
Labaune, C., Jouet, G., Berné, S., Gensous, B., Tesson, M., Delpeint, A., 2005. Seismic stratigraphy of the Deglacial deposits of the Rhone prodelta and of the adjacent shelf. Marine Geology, 222-223, 299-311.
Lambeck, K., Bard, E., 2000. Sea-level change along the French Mediterranean coast for the past 30 000 years. Earth and Planetary Science Letters, 175, 203-222.
Lambeck, K., Yokoyama, Y.Purcell, T., 2002. Into and out of the Last Glacial Maximum: sea-level change during Oxygen Isotope Stages 3 and 2. Quaternary Science Reviews, 21, 343-360.
Lofi, J., Gorini, C., Berne, S., Clauzon, G., Tadeu Dos Reis, A., Ryan, W.B.F., Steckler, M.S., 2005. Erosional processes and paleo-environmental changes in the Western Gulf of Lions (SW France) during the Messinian Salinity Crisis. Marine Geology, 217, 1-30.
Magny, M., Miramont, C., Sivan, O., 2002. Assessment of the impact of climate and anthropogenic factors on Holocene Mediterranean vegetation in Europe on the basis of palaeohydrological records. Palaeogeography, Palaeoclimatology, Palaeoecology, 186, 47-59.
Magny, M., Aalbersberg, G., Begeot, C., Benoit-Ruffaldi, P., Bossuet, G., Disnar, J.-R., Heiri, O., Laggoun-Defarge, F., Mazier, F., Millet, L., 2006. Environmental and climatic changes in the Jura mountains (eastern France) during the Lateglacial-Holocene transition: A multi-proxy record from Lake Lautrey. Quaternary Science Reviews, 25, 414-445.
Marsset, T., Bellec, V., 2002. Late Pleistocene-Holocene deposits of the Rhône inner continental shelf (France): detailed mapping and correlation with previous continental and marine studies. Sedimentology, 49, 255-276.
Millot, C., 1987. Circulation in the Western Mediterranean Sea. Oceanologica Acta, 10, 143-149.
Millot, C., 1999. Circulation in the Western Mediterranean Sea. Journal of Marine Systems, 20, 423-442.
Posamentier, H.W., Allen, G.P., James, D.P., Tesson, M., 1992. Forced regressions in a sequence stratigraphic framework: concepts, examples and exploration significance. American Association of Petroleum Geologists Bulletin, 76, 1687-1709.
Provansal, M., Vella, C., Arnaud-Fassetta, G., Sabatier, F., Maillet, G., 2003. Role of fluvial sediment inputs in the mobility of the Rhône delta coast (France). Géomorphologie: relief, processus, environnement, 4, 271-282.
Rabineau, M., Berne, S., Aslanian, D., Olivet, J.-L., Joseph, P., Guillocheau, F., Bourillet, J.-F., Ledrezen, E., Granjeon, D., 2005. Sedimentary sequences in the Gulf of Lion: A record of 100,000 years climatic cycles. Marine and Petroleum Geology, 22, 775-804.

Reimer, P.J., Baillie, M.G.L., Bard, E., Bayliss, A., Beck, J.W., Bertrand, C.J.H., Blackwell, P.G., Buck, C.E., Burr, G.S., Cutler, K.B., Damon, P.E., Edwards, R.L., Fairbanks, R.G., Friedrich, M., Guilderson, T.P., Hogg, A.G., Hughen, K.A., Kromer, B., McCormac, F.G., Manning, S.W., Ramsey, C.B., Reimer, R.W., Remmele, S., Southon, J.R., Stuiver, M., Talamo, S., Taylor, F.W., van der Plicht, J., Weyhenmeyer, C.E., 2004. IntCal04 Terrestrial radiocarbon age calibration. Radiocarbon, 46, 1029-1058.

Roberts, H.H., Fillon, R.H., Kohl, B., Robalin, J.M., Sydow, J.C., 2004. Depositional architecture of the Lagniappe delta:sediment characteristics, timing of depositional events, and temporal relationship with adjacent shelf-edge deltas. In: J.B. Anderson and R.H. Fillon (Editors), Late Quaternary Stratigraphic evolution of the northern Gulf of Mexico margin. SEPM (Society for Sedimentary Geology), Tulsa, pp. 143-188.

Ryan, W.B.F., Cita, M.B., 1978. The nature and distribution of Messinian erosional surface-indication of a several kilometer-deep Mediterranean in the Miocene. Marine Geology, 27, 193-230.

Sabatier, F., Maillet, G., Provansal, M., Fleury, T.-J., Suanez, S., Vella, C., 2006. Sediment budget of the Rhone delta shoreface since the middle of the 19th century. Marine Geology, 234, 143-157.

Skinner, L.C., McCave, I.N., 2003. Analysis and modelling of gravity- and piston coring based on soil mechanics. Marine Geology, 199, 181-204.

Stuiver, M., Reimer, P.J., 1993. Extended 14C database and revised CALIB radiocarbon calibration program. Radiocarbon, 35, 215-230.

Taviani, M., Roveri, M., Impiccini, R., Vigliotti, L., 1998. Segnalazione di Quaternario marino nella Val Chero (Appennino Piacentino). Bollettino della Società Paleontologica Italiana 36, 331-338

Tesson, M., Gensous, B., Naudin, J.-J., Chaignon, V.Bresoli, J., 1998. Carte morpho-bathymétrique de la plate-forme du golfe du Lion: un outil pour la reconnaissance et l'analyse des modifications environnementales récentes. Comptes Rendus de l'Academie des Sciences - Series IIA - Earth and Planetary Science, 327, 541-547.

Trincardi, F., Cattaneo, A., Correggiari, A., Langone, L., 1996. Stratigraphy of the late-Quaternary deposits in the central Adriatic basin and the record of short-term climatic events In: P. Guilizzoni and F. Oldfield (Editors), Palaeoenvironmental analysis of Italian crater lake and Adriatic sediments. Mem. Ist. Ital. Idrobiol., pp. 39-70.

Trincardi, F., Cattaneo, A., Correggiari, A., 2004. Mediterranean prodelta systems: natural evolution and human impact investigated by Eurodelta. Oceanography, 17, 34-45.

Van Wagoner, J.C., Mitchum, R.M., Campion, K.M., Rahmanian, V.D., 1990. Siliciclastic sequence stratigraphy in well logs, cores and outcrops. Methods in Exploration Series N° 7. American Association of Petroleum Geologists, 55 pp.

Vella, C., 1999. Perception et évaluation de la mobilité du littoral holocène sur la marge orientale du delta du Rhône. PhD Thesis, Aix-Marseille 1, Aix, 225 pp.

Vella, C., Fleury, T.-J., Raccasi, G., Provansal, M., Sabatier, F.Bourcier, M., 2005. Evolution of the Rhone delta plain in the Holocene. Marine Geology, 222-223, 235-265.

Walker, R.G.Plint, A.G., 1992. Wave- and storm- dominated shallow marine systems. In: R.G. Walker and N.P. James (Editors), Facies Models - Response to Sea Level Changes. Geological Association of Canada, St John, pp. 219-238.

Figure captions

Fig. 1: General bathymetric map of the Gulf of Lions (based on Berné et al. (2001)). The distribution of sand is modified from Aloïsi (1986). Isobath contour line interval is 5 m from 0 to 150 m water depth, 200 m beyond 150 m. The arrow represents the direction of the Northern contour current. LDC: Lacaze-Duthiers Canyon; PvC: Pruvot Canyon; AC: Aude Canyon (or Bourcart canyon); HC: Hérault Canyon; SC: Sète Canyon; MaC: Marti Canyon; PRC: Petit Rhône Canyon; GRC: Grand Rhône Canyon; EC: Estaque Canyon.

Fig. 2: Seismic (chirp) section STch 93 across the western Rhône subaqueous deltaic complex (modified from Berné et al. (2004)). The sandy upper shoreface (upper part of unit U400) forms a step well visible on the detailed bathymetric map (see Fig. 3). Note the very exaggerated vertical scale. CS:

Cemented sands. Units including U300 through U500 represent the trangressive and highstand deposits that are studied in this paper. “1” and “2” are close-up views of unit U400. ”m”: multiple. D70, D60, D50 and D45 are surfaces of subaerial erosion that formed during Marine Isotope Stages 2, 6, 8 and 10, respectively. They bound regressive or “falling stage” systems tracts.

Fig. 3: Detailed morphology of the Rhône subaqueous delta and main morpho-sedimentary features offshore and onshore. This map is based on the compilation of sounding charts from the French Hydrographic Service of the Navy (SHOM). Contour lines are every 50 cm in order to highlight morphologic features. The thick arrow corresponds to the boundary between two Digital Terrain Models, that generate an artifact along the –50 m contour line (see text for explanation). The deglacial retreat path of the Rhône from the Petit Rhône canyon head (PRC) can be inferred with, from South to North: (1), (2) and (3): lowstand and early transgressive shorelines and/or delta fronts; (4): retreat path of the Rhône presumably during MWP1A; (4w1), (4w2), and (4e) correspond to the retreat path of other Rhône distributaries. (5): sandy delta front of the Early Rhône Deltaic Complex; 6: remnants of the Early St Ferreol delta; (7): remnants of a Peccais (?) delta front; (8): remnants of a Little Ice Age delta front (Bras de Fer); (9): remnants of the Peygoulier delta front; (10): modern Roustan delta front. The modern delta plain exhibits two distributaries, the “Petit Rhône” (little Rhône) to the west and the “Grand Rhône” (large Rhône) to the east. STKS25, MD992352 BMVK06, and BMKS16 are cores described or mentioned in the text. Paleo-shorelines, sand ridges and onshore deltaic lobes (in red) are from L’Homer et al. (1981), Arnaud-Fassetta (1998), Vella (1999), Provansal (2003). Sand distribution is based on Aloïsi (1986), modified according to our samples.

Fig. 4: Slope map calculated from the Digital Terrain Model shown in Fig. 3. Note the steep slope of the modern Rhone prodelta compared to older lobes. Legend is the same as for Fig. 3.

Fig. 5: Swath bathymetric (EM1000 and EM 300) map of part of the Early Rhône Deltaic Complex (position in Fig. 3). Note elongated NW-SE ridges (interpreted as beach ridges), slightly oblique relative to present bathymetric contour lines, with superimposed subaqueous N-S sand dunes (possibly active during extreme events).

Fig. 6: Sparker profile BAS1-38 across the western Rhône subaqueous delta (position in Fig. 3). The location and actual penetration depth (with vertical scale in m) of cores MD992352 and BMKS16 is shown. The difference in core lengths is explained by different lithologies: clayey silt for the bottomsets, fine to medium sand for the topsets. Sequences and surfaces are the same as in Figure 2.

Fig. 7. Chirp seismic data from the upper chaotic facies (1) and the lower clinoform facies (2) (position in Fig. 3).

Fig. 8: Lithologic description and photographs of cores BMVK06 and MD992352 (positions in Figs. 3 and 6). For clarity, different vertical scales are used. Calibrated ages of dated samples (stars) are also reported.

Fig. 9: Photograph of the upper part of core KSTR25 (position in Fig. 3) with cobbles and pebbles (water depth at -55mbmsl).

Fig. 10: Age model curve for core MD992352, with 1 sigma error bars. Numbered lozenges represent the position along clinoforms of Figure 11 (the corresponding ages are reported in table 2). Only dates below the erosion surface D500 are taken into account, the time span represented by this surface being unknown.

Fig. 11: Part of Chirp seismic profile STch93. Core length is converted into milliseconds using an average sonic velocity of 1580 m/s (as measured in the core). The coarse lag observed between 1 m and 1.20 m on the core corresponds to the erosion surface named D500 on the seismic profile, implying that the upper 50 cm of sediment was lost during the coring operation. The lower coarse lag situated at the bottom of the core matches the depth of the ravinement surface (D350) seen on seismic profiles. X symbols correspond to the boundary between deltaic and prodeltaic seismic facies (see text and Fig. 7 for explanation), numbers are used for identification of clinoforms.

Fig. 12: Chirp seismic profile STch123 (strike section, position in Fig. 3). Note the chaotic seismic facies that underlies D350 (the ravinement surface). D400 is positioned by crossing with sparker profiles where downlap termination are seen more clearly than on chirp profiles.

Fig. 13: Schematic representation of the Early Rhone Deltaic Complex transgressive parasequence, with key components and corresponding chronology of deposition. This complex consists of an aggrading/retrograding unit (U350) topped by a prograding unit (U400). U350 formed during a period of rapid sea-level rise (the Bølling-Allerød, noted B/A, including Melt Walter Pulse 1A, noted MWP1A). The transition between aggradation and progradation corresponds to the onset of the Younger Dryas (YD), a phase of decreased sea-level rise. Progradation of U400 occurred during YD, but was maintained during the Preboreal (PB) due to high sediment supply, until about 10,500 yr cal BP. It is a downlap surface named Maximum Transgression Surface (MTS) in the senses of Helland-Hansen and Martinsen (1996). This complex represents a transgressive parasequence bounded by flooding surfaces (FS1 and FS2). Note that none of the key surfaces or units is in phase with sea-level changes, except for MTS which corresponds to the onset of the Younger Dryas. The sea-level curve is from Bard et al. (1996).

Fig. 14: Relative sea-level curve in the Gulf of Lions for the last 20 kyr. The point at -99 m below present sea-level is from Bassetti et al. (2006), the one between -110 and -115 m is from Jouet et al. (2006). Our data are not corrected from isostatic effects and are therefore relative sea-levels.

Table 1: Summary of the dated samples used for this study. Absolute dates were obtained with accelerator mass spectrometer (AMS) ^{14}C dating of well-preserved shells and microfauna. They were made at Lawrence Livermore National Laboratory (LLNL), and at Poznan Radiocarbon Laboratory (PRL). The ages reported herein are delta ^{13}C-normalised conventional ^{14}C years. For ages between 0 and 21,880 yr 14C BP, calendar (i.-e. calibrated) ages were calculated using the Calib 5.0 sofware (Stuiver and Reimer, 1993). For marine material, the Marine04 calibration curve (Hughen et al., 2004) was used with no deviation from the average reservoir age (-408 years). For continental material (namely the organic debris of the St Ferreol prodelta) the Intcal04 calibration curve (Reimer et al., 2004) was used.

Table 2: Average age of clinoforms of Figure 11 (using the age model of Fig. 10) and depth of the deltaic/shoreface to prodeltaic transition (black crosses in Fig. 11), using a sonic velocity of 1580 m/s in sediment.

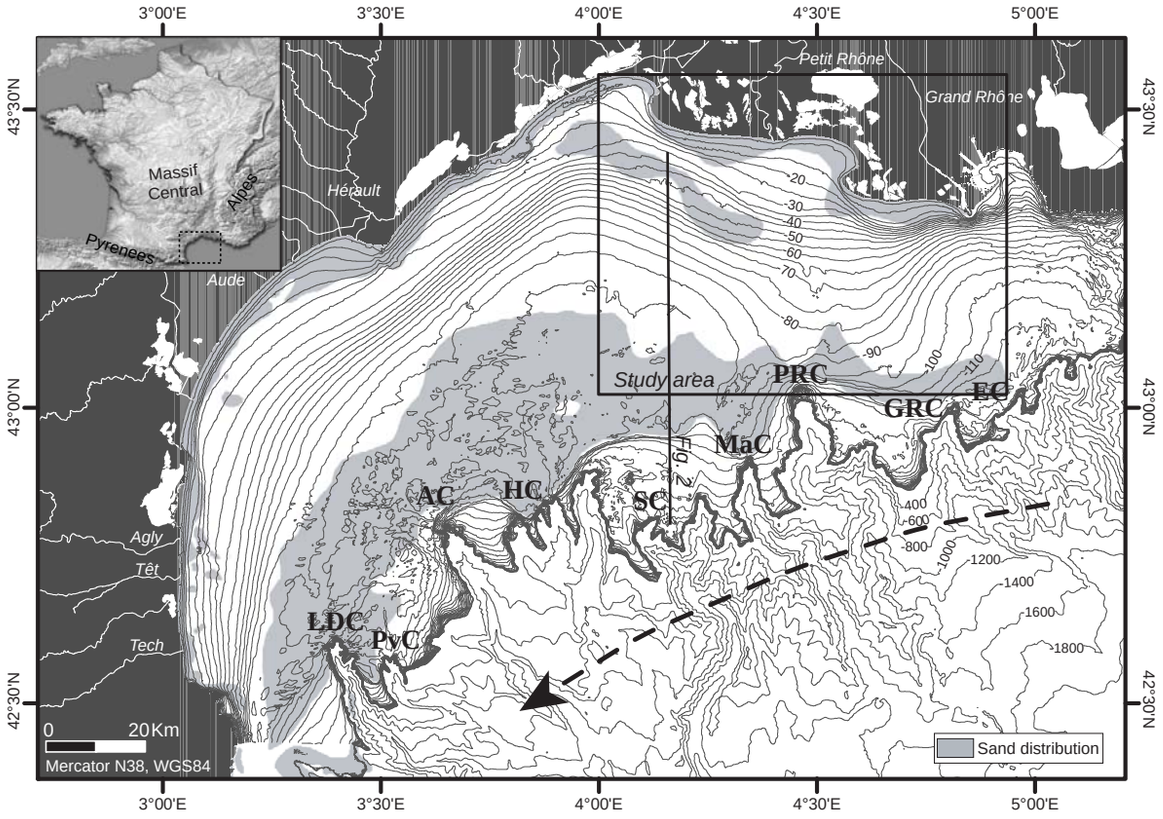

Fig. 1 Berné et al.

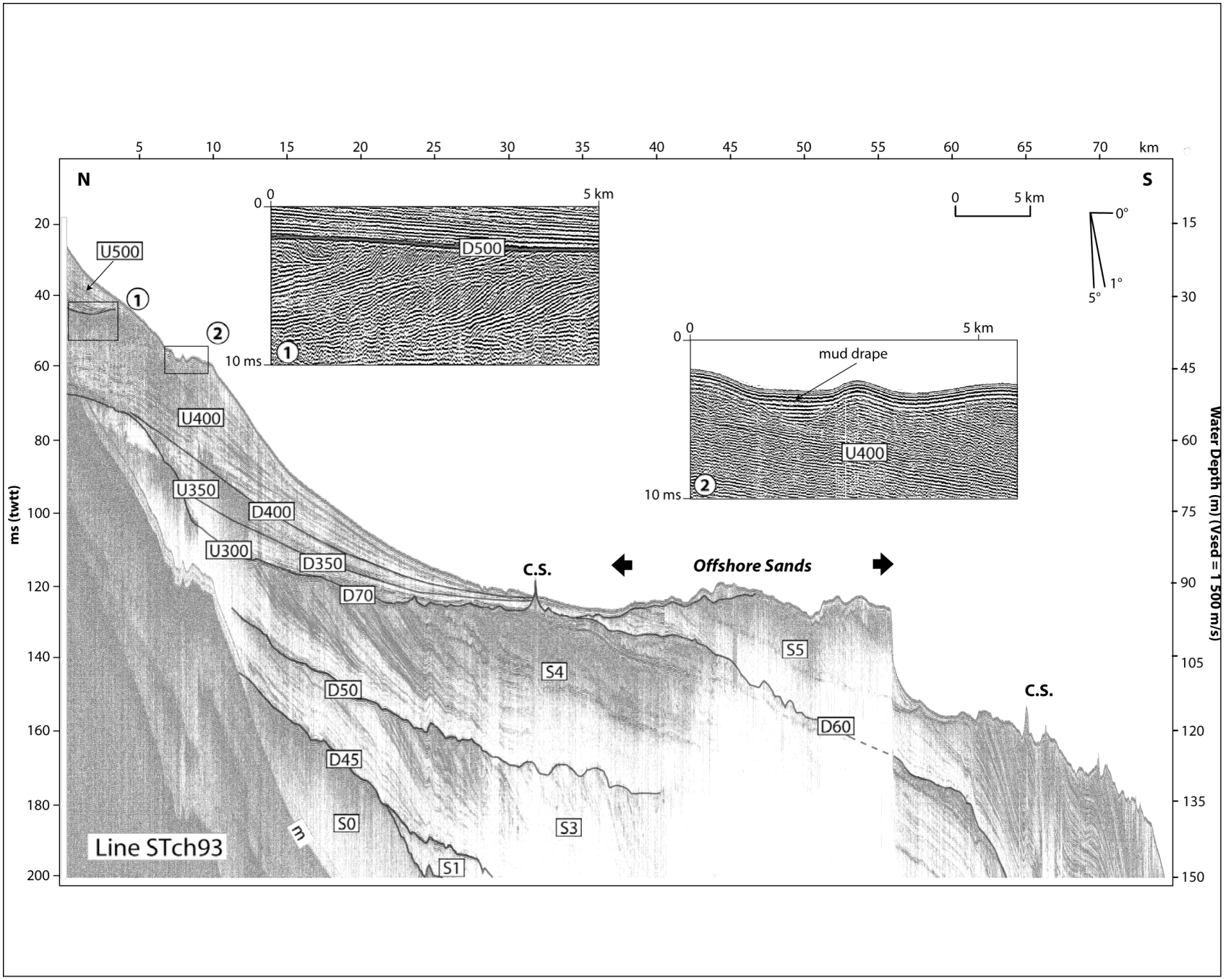

Fig. 2 Berné et al.

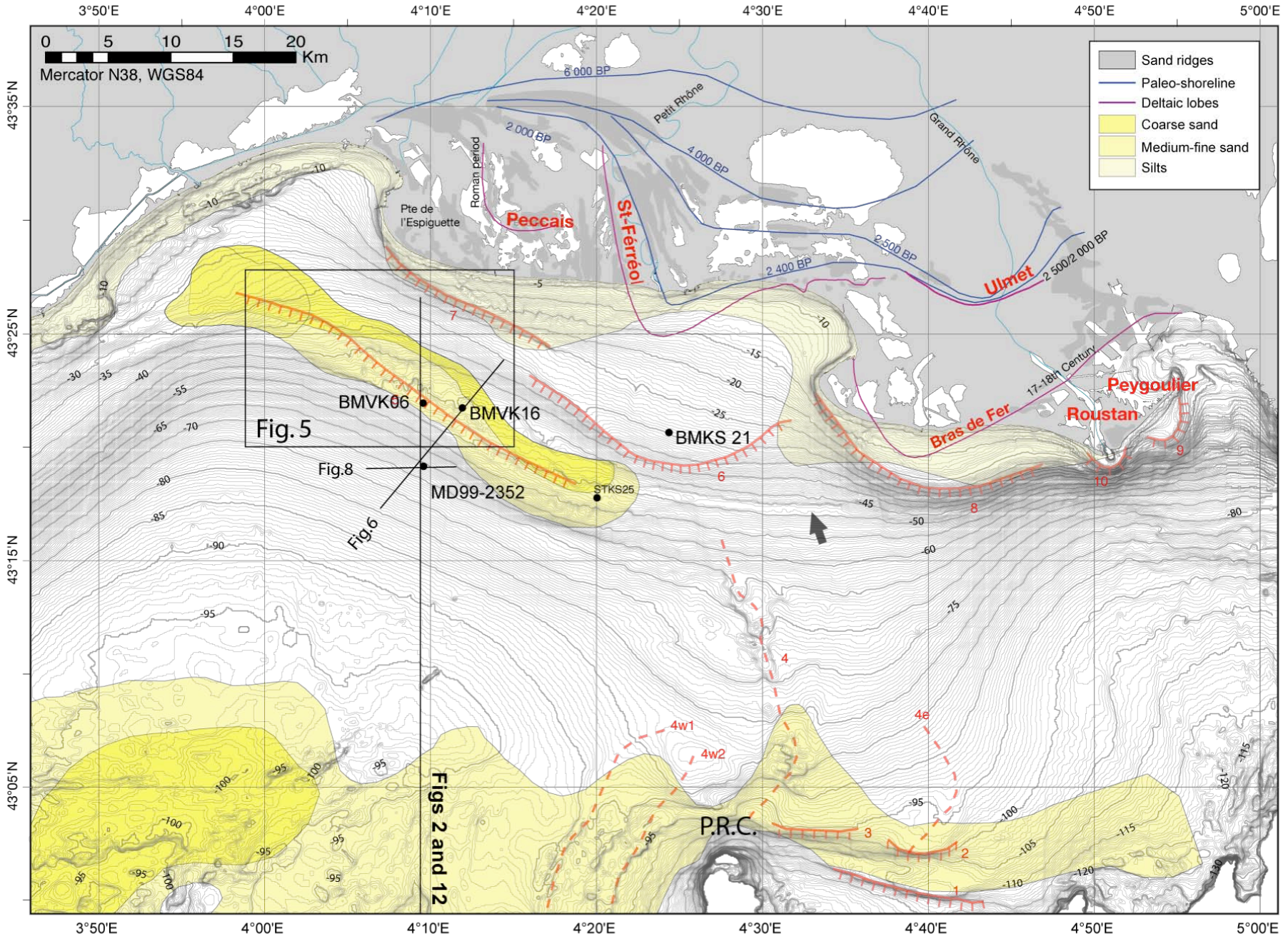

Fig. 3: Berné et al.

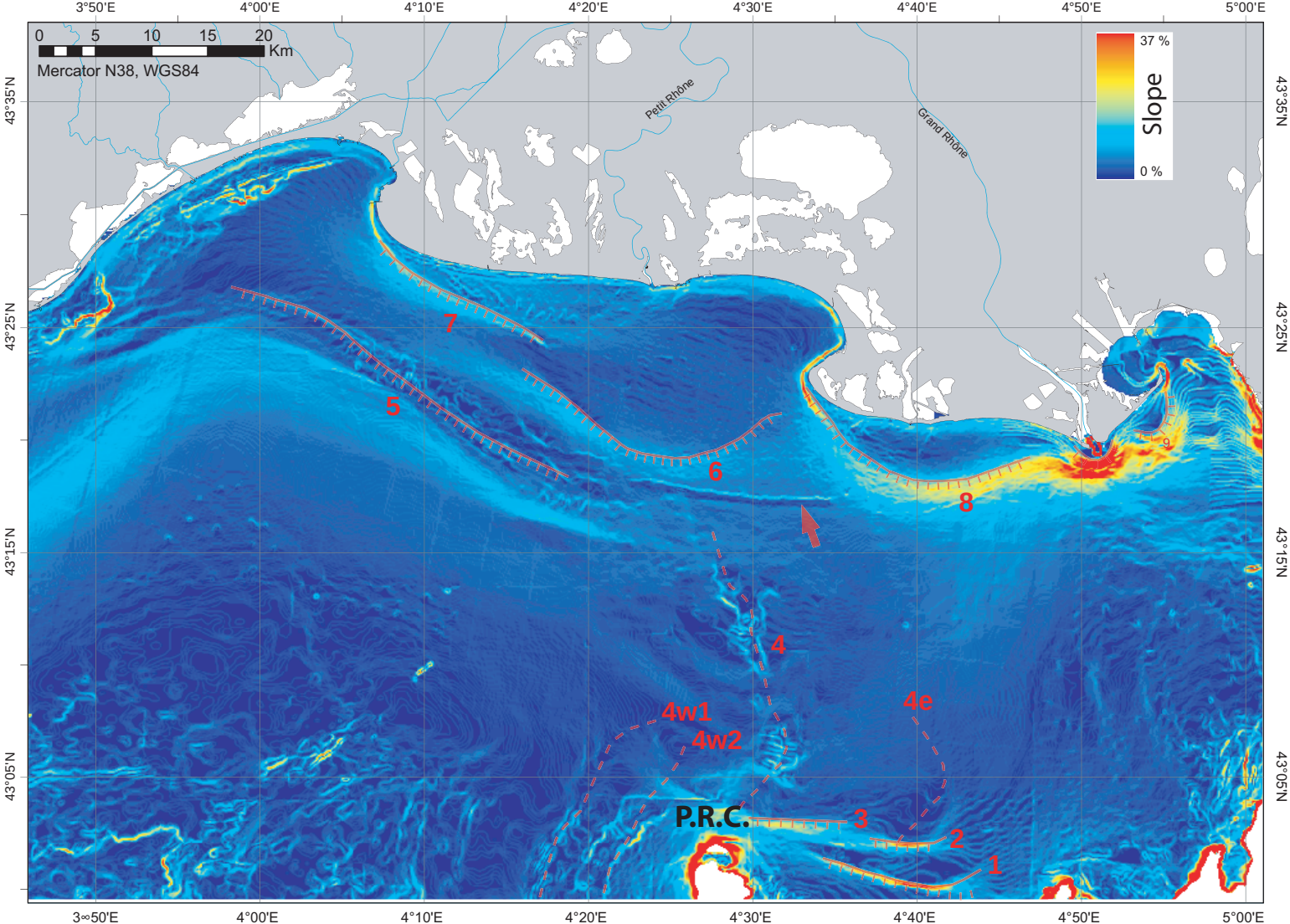

Fig. 4 Berné et al.

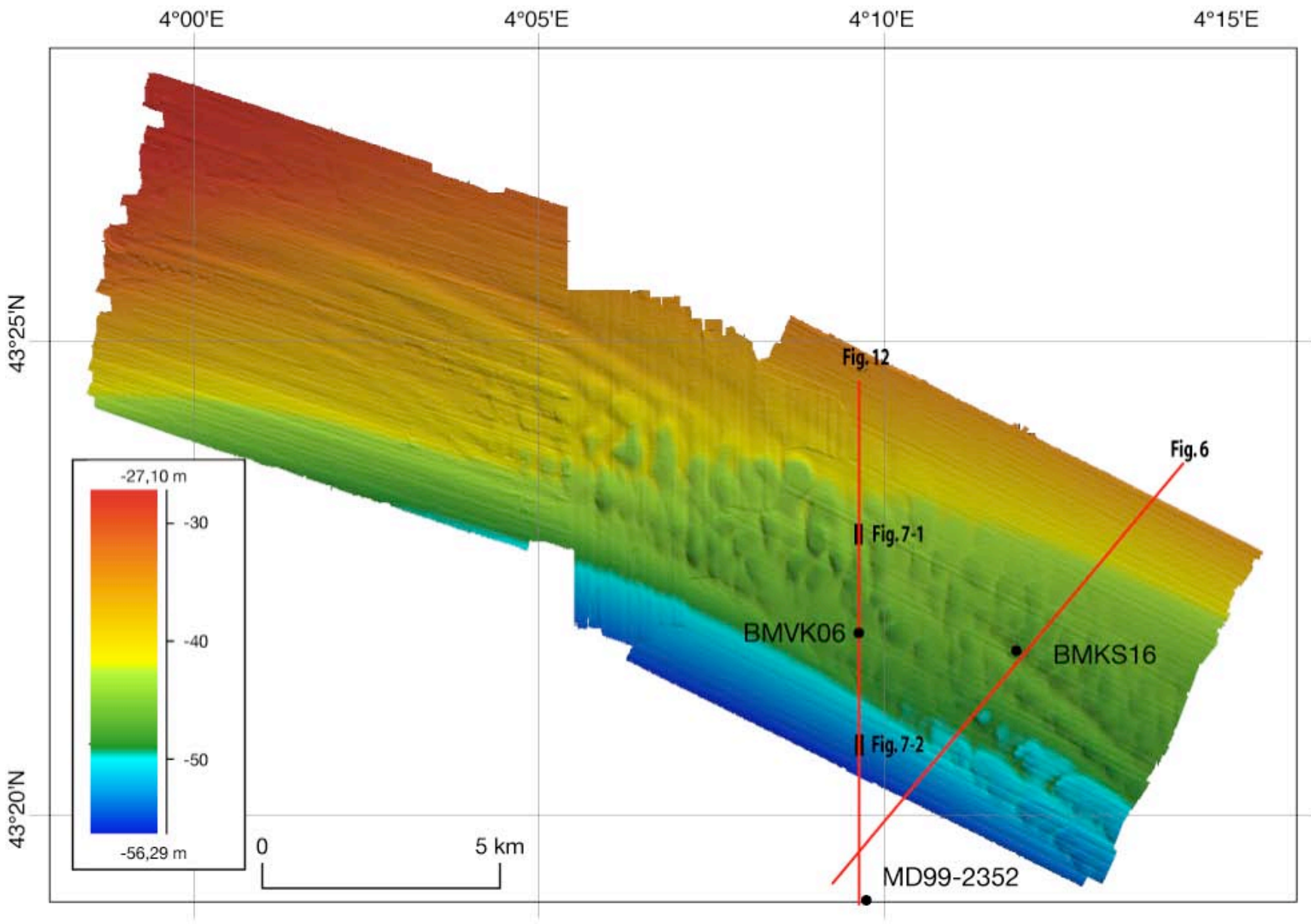

Fig. 5 Berné et al.

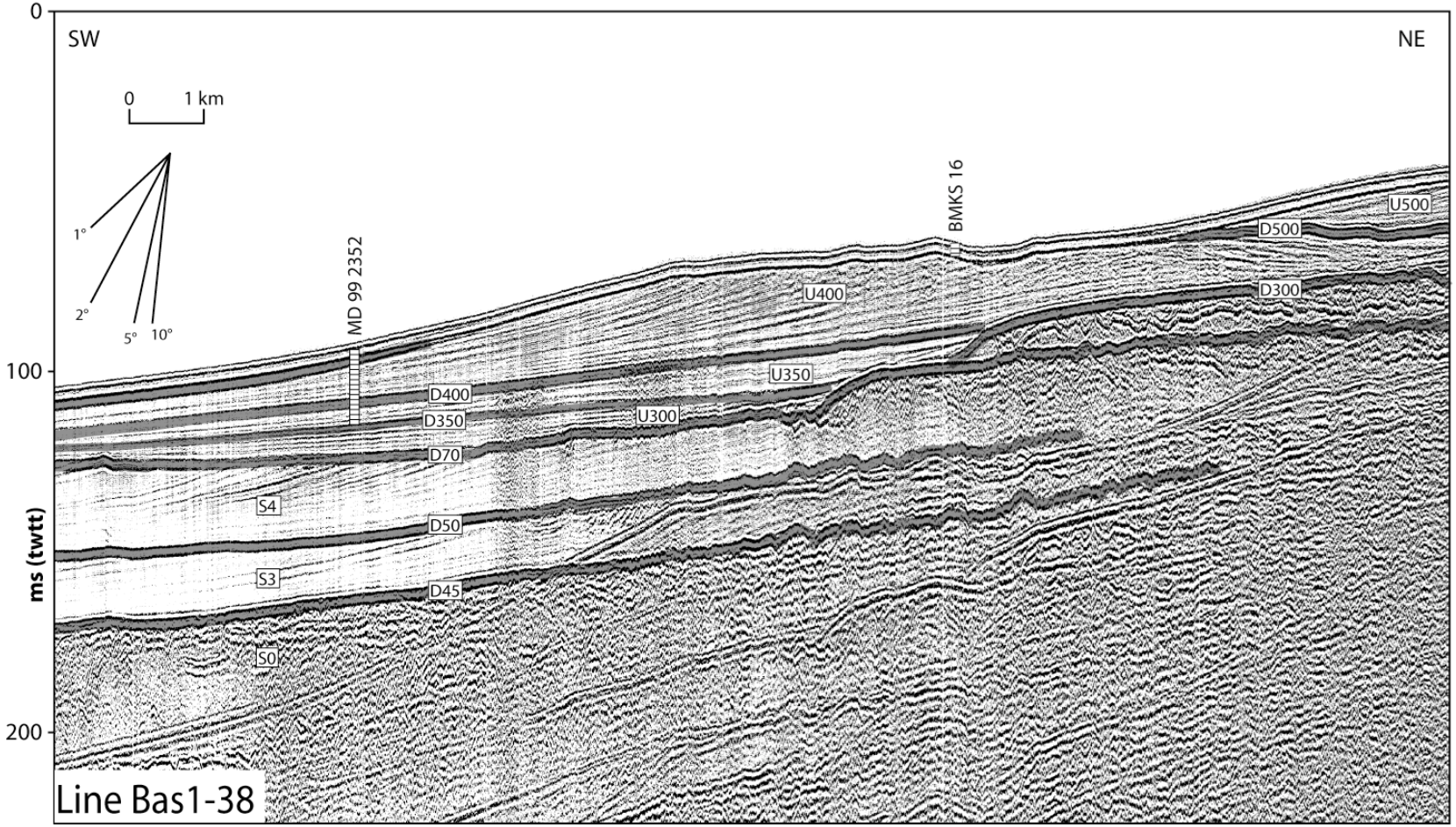

Fig. 6 Berné et al

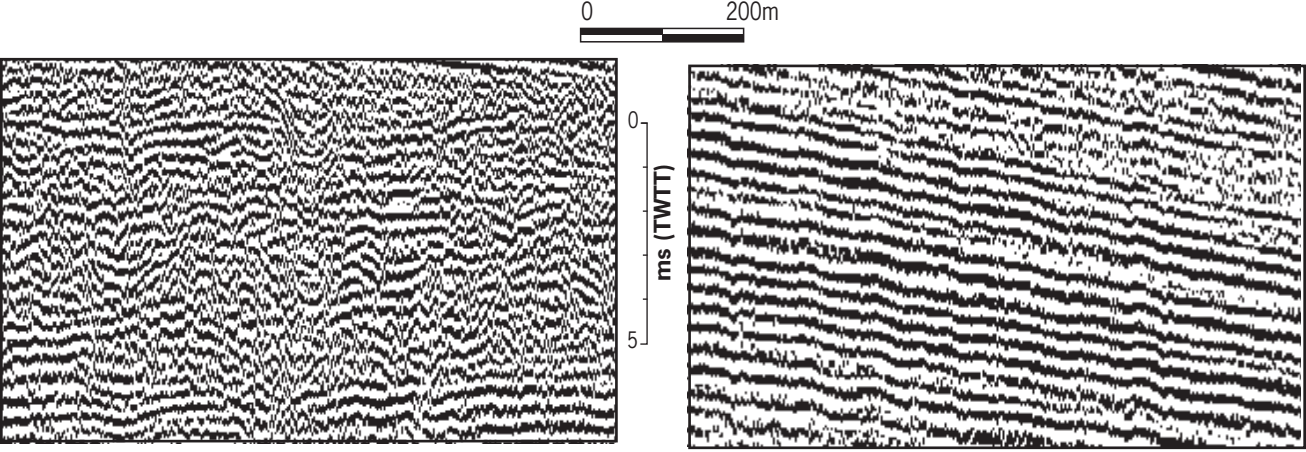

1- upper chaotic facies

2- lower clinoform facies

Fig.7 Berné et al.

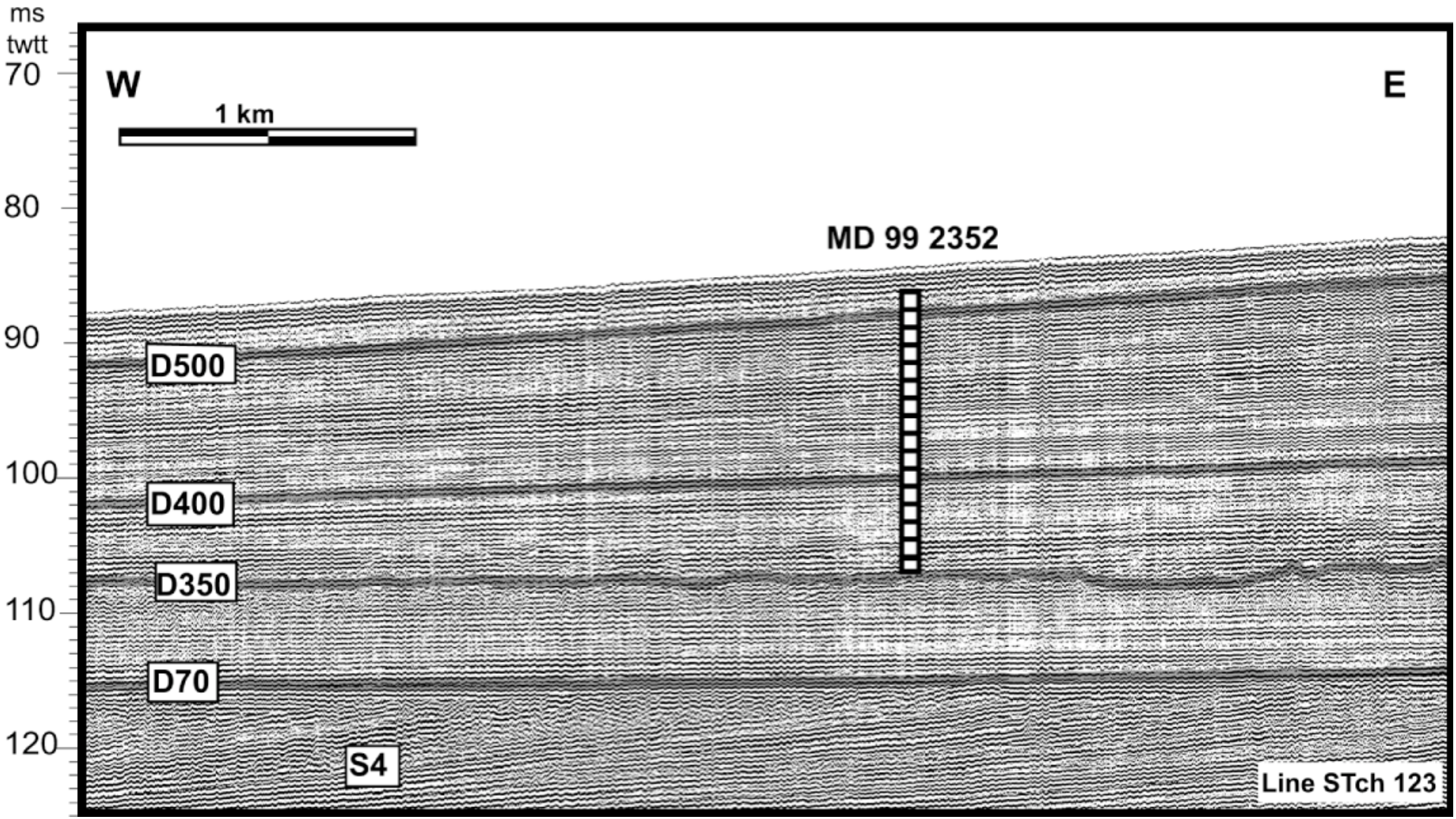
ms
twtt
70
80
90
100
110
120
W
E
1 km
MD 99 2352
D500
D400
D350
D70
S4
Line STch 123

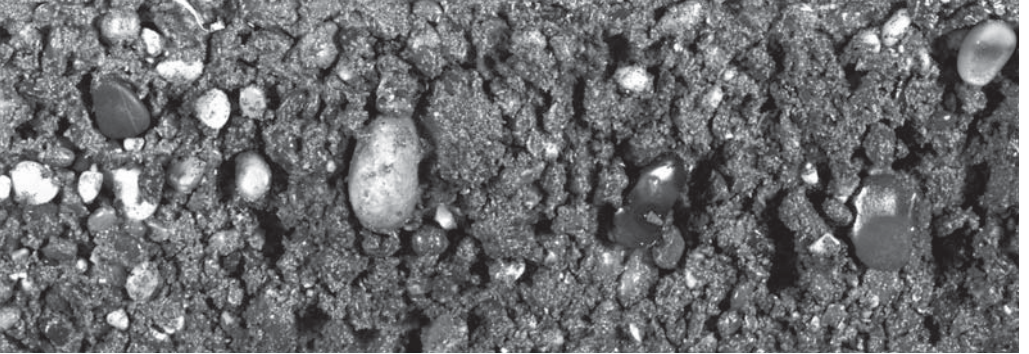

Fig. 9 Berné et al.

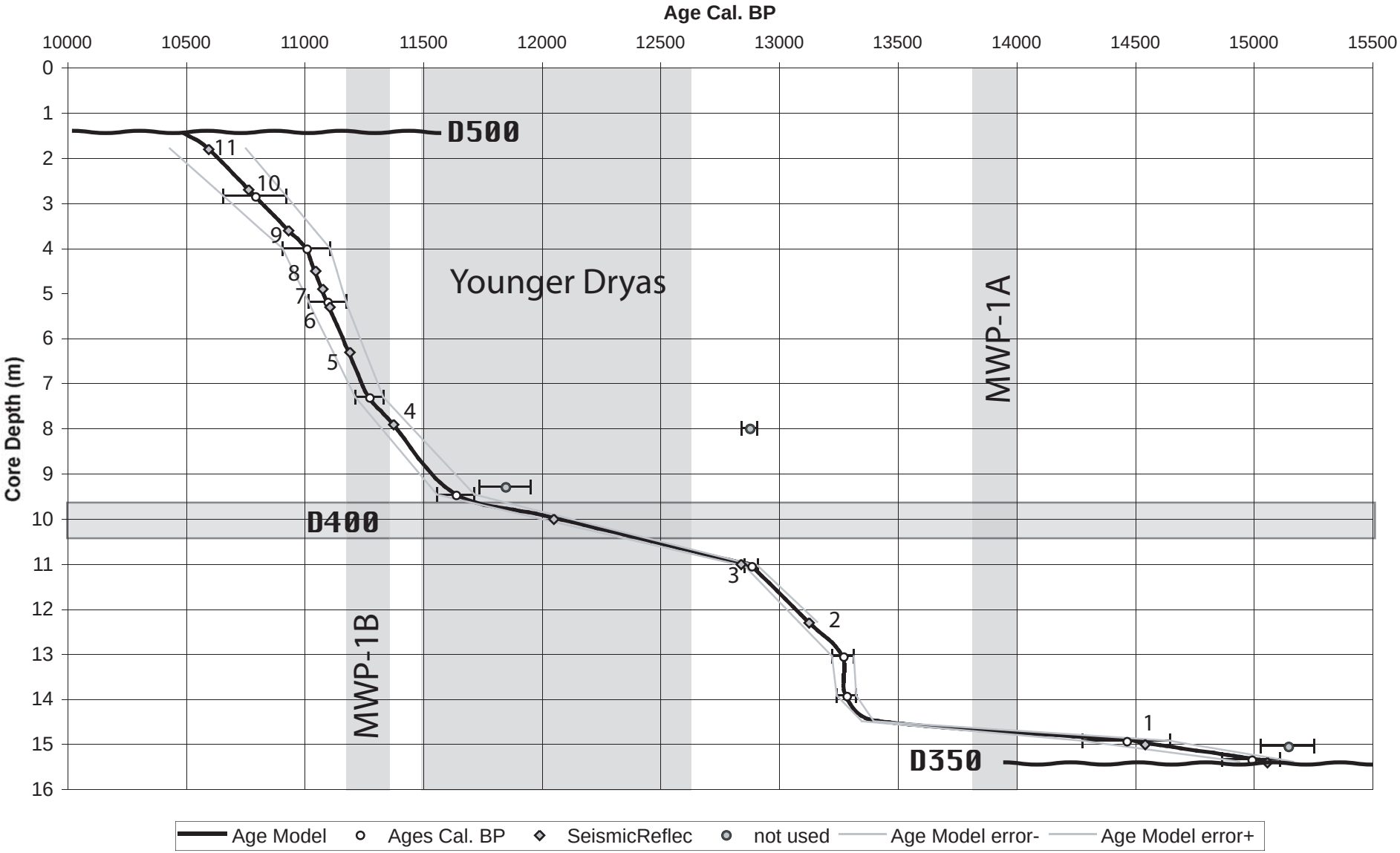

Figure 10 Berné et al.

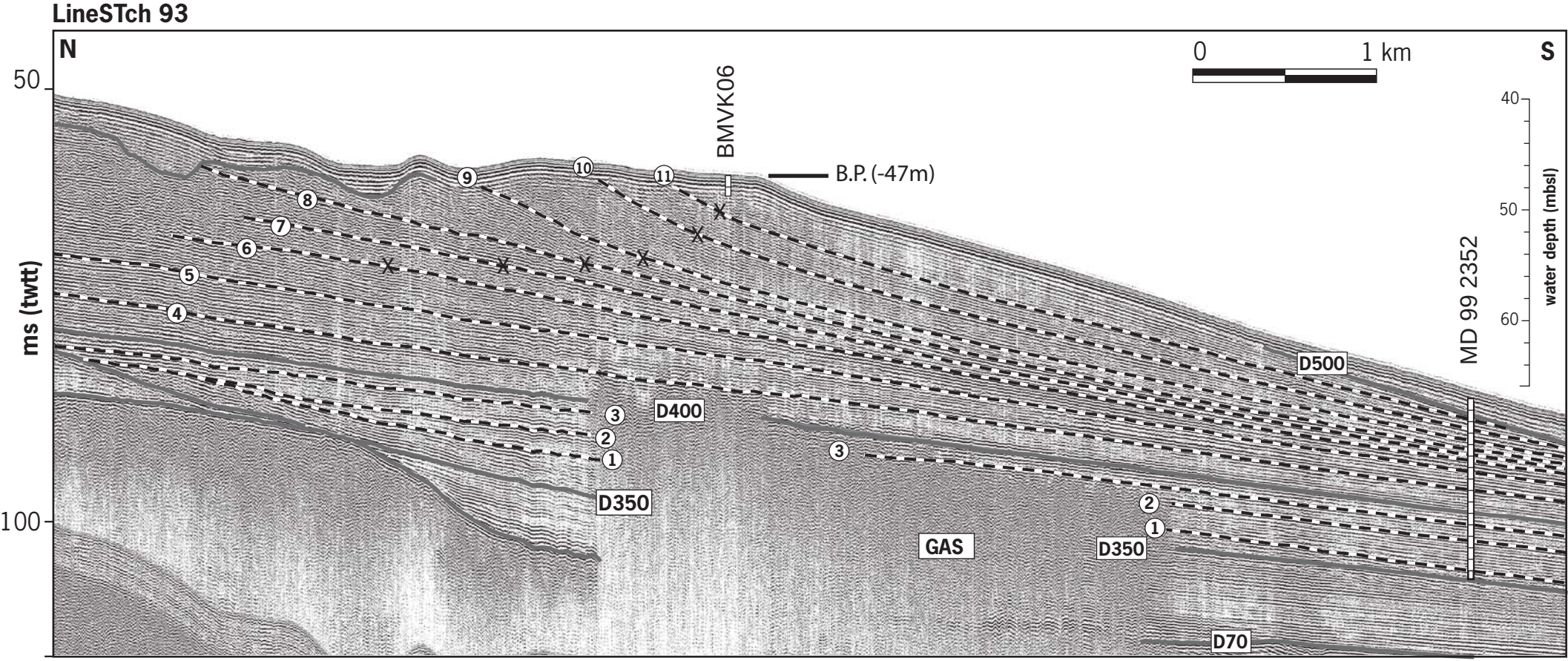

Fig. 11 Berné et al.

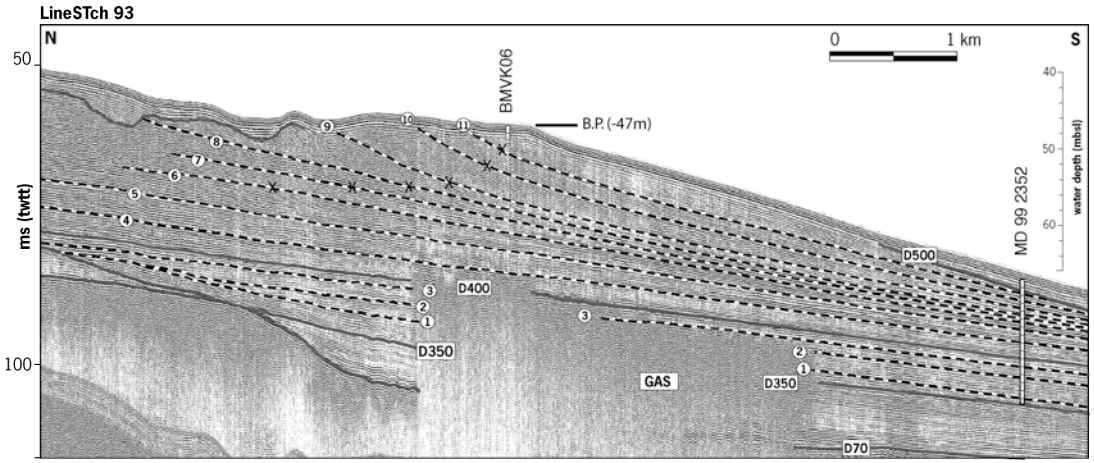

New Fig. 12 Berné et al.

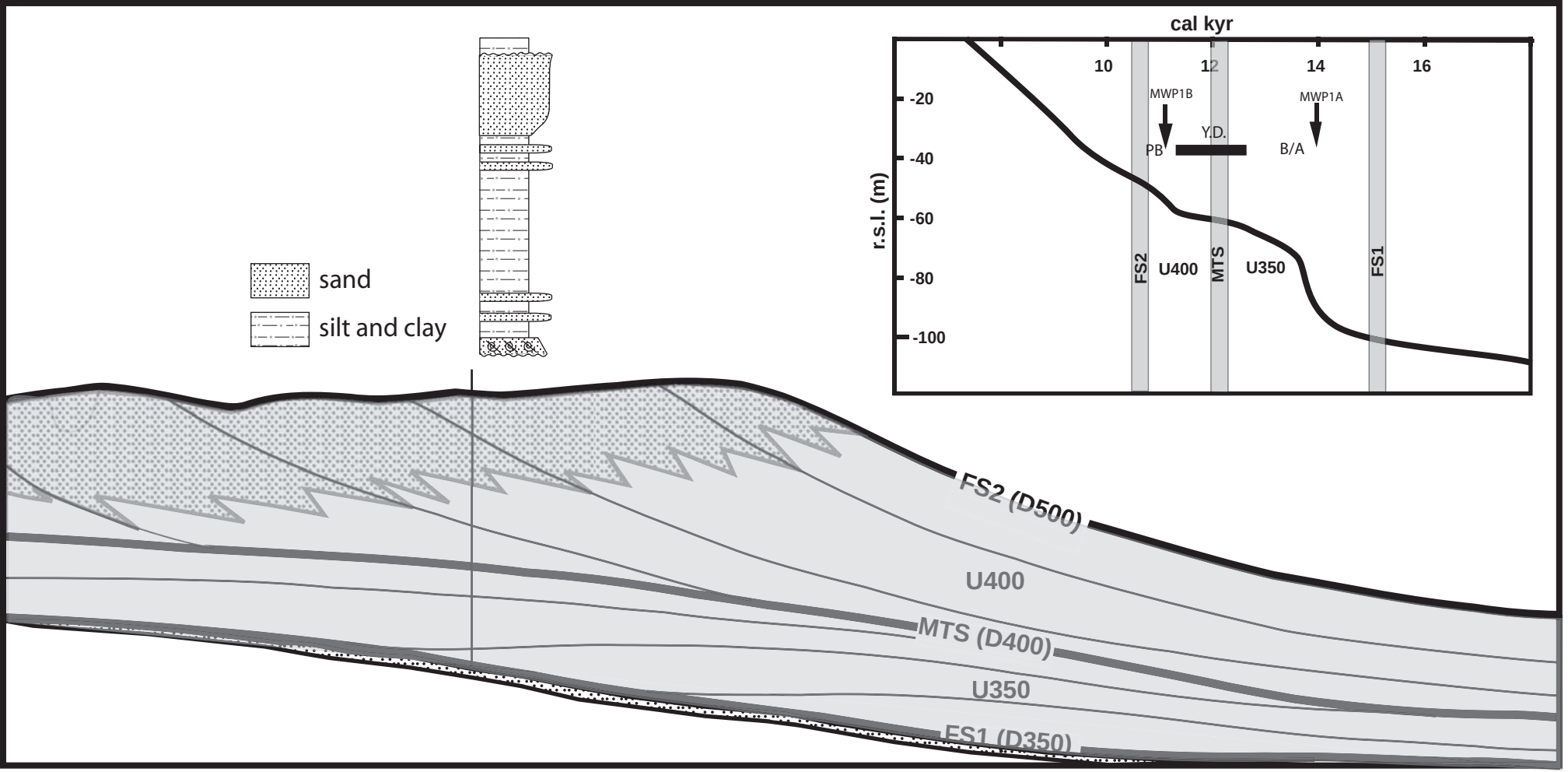

Fig. 13 Berné et al.

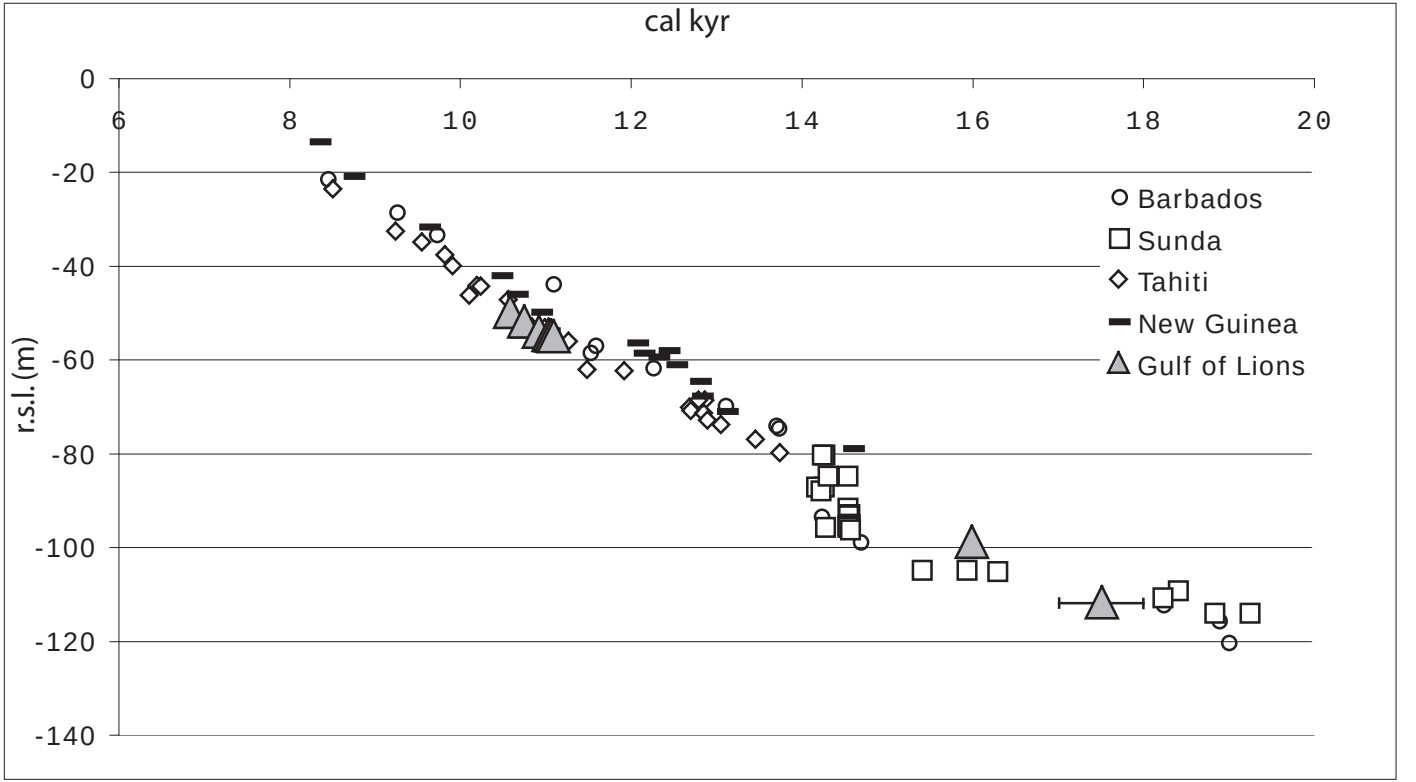

Fig. 14 Berné et al.